

# Synchronization of Kuramoto Oscillators via Cutset Projections

Saber Jafarpour, *Member, IEEE*, and Francesco Bullo, *Fellow, IEEE*

**Abstract**—Synchronization in coupled oscillators networks is a remarkable phenomenon of relevance in numerous fields. For Kuramoto oscillators the loss of synchronization is determined by a trade-off between coupling strength and oscillator heterogeneity. Despite extensive prior work, the existing sufficient conditions for synchronization are either very conservative or heuristic and approximate. Using a novel cutset projection operator, we propose a new family of sufficient synchronization conditions; these conditions rigorously identify the correct functional form of the trade-off between coupling strength and oscillator heterogeneity. To overcome the need to solve a nonconvex optimization problem, we then provide two explicit bounding methods, thereby obtaining (i) the best-known sufficient condition for unweighted graphs based on the 2-norm, and (ii) the first-known generally-applicable sufficient condition based on the  $\infty$ -norm. We conclude with a comparative study of our novel  $\infty$ -norm condition for specific topologies and IEEE test cases; for most IEEE test cases our new sufficient condition is one to two orders of magnitude more accurate than previous rigorous tests.

**Index Terms**—Kuramoto oscillators, frequency synchronization, synchronization manifold, cutset projection.

## I. INTRODUCTION

*a) Problem description and literature review:* The phenomenon of collective synchronization appears in many different disciplines including biology, physics, chemistry, and engineering. In the last few decades, many fundamental contributions have been made in providing and analyzing suitable mathematical models for synchronizations of coupled oscillators [45], [46]. Much recent interest in studying synchronization has focused on systems with finite number of oscillators coupled through a nontrivial topology with arbitrary weights. Consider a system consists of  $n$  oscillators, where the  $i$ th oscillator has a natural rotational frequency  $\omega_i$  and its dynamics is described using the phase angle  $\theta_i \in \mathbb{S}^1$ . When there is no interaction between oscillators, the dynamics of  $i$ th oscillator is governed by the differential equation  $\dot{\theta}_i = \omega_i$ . One can model the coupling between oscillators using a weighted undirected graph  $G$ , where the interaction between oscillators  $i$  and  $j$  is proportional to  $\sin$  of the phase difference between angles  $\theta_i$  and  $\theta_j$ . This model, often referred to as the Kuramoto model, is one of the most widely-used model for studying synchronization of finite population of coupled oscillators. The Kuramoto model and its generalizations appear in various applications including the study of pacemaker cells

in heart [31], neural oscillators [8], deep brain simulation [41], spin glass models [25], oscillating neutrinos [36], chemical oscillators [26], multi-vehicle coordination [39], synchronization of smart grids [17], security analysis of power flow equations [4], optimal generation dispatch [28], and droop-controlled inverters in microgrids [10], [40].

Despite its apparent simplicity, the Kuramoto model gives rise to very complex and fascinating behaviors [16]. A fundamental question about the synchronization of coupled-oscillators networks is whether the network achieves synchronization for a given set of natural frequencies, graph topology, and edge weights. While various notions of synchronization in Kuramoto models have been proposed, phase synchronization and frequency synchronization are arguably the most fundamental. A network of coupled oscillators is in phase synchronization if all the oscillators achieve the same phase and it is in frequency synchronization if all the oscillators achieve the same frequency. While phase synchronization is only achievable for uniform frequencies irrespective of the network structure [24], [39], [33], frequency synchronization in Kuramoto oscillators is possible for arbitrary frequencies, but depends heavily on the network topology and weights.

*b) Prior sufficient or necessary conditions for frequency synchronization:* Frequency synchronization of Kuramoto oscillators has been studied using various approaches in different scientific communities. In the physics and dynamical systems communities, in the limit as number of oscillators tends to infinity, the Kuramoto model is analyzed as a first-order continuity equation [27], [18]. In the control community, much interest has focused on the finite numbers of oscillators and on connections with graph theory. The first rigorous characterization of frequency synchronization is developed for the complete unweighted graphs [2], [32], [42]. The works [2], [32] present implicit algebraic equations for the threshold of synchronization together with local stability analysis of the synchronization manifolds. The same set of equations has been reported in [42, Theorem 3], where a bisection algorithm is proposed to compute the synchronization threshold. Moreover, [43, Theorem 4.5] presents a synchronization analysis for complete unweighted bipartite graphs. Via nonsmooth Lyapunov function methods, [12, Theorem 4.1] characterizes the case of complete unweighted graphs with arbitrary frequencies in a fixed compact support. For acyclic graphs a necessary and sufficient condition for frequency synchronization is presented in [24, Remark 10] and [17, Theorem 2]. Inspired by this characterization for acyclic graphs and using an auxiliary fixed-point equation, a sufficient condition for synchronization of ring graphs is proved in [17, Theorem 3, Condition 3].

This work was supported in part by the U.S. Department of Energy (DOE) Solar Energy Technologies Office under Contract No. DE-EE0000-1583.

Saber Jafarpour, and Francesco Bullo are with the Mechanical Engineering Department and the Center of Control, Dynamical-Systems and Computation, UC Santa Barbara, CA 93106-5070, USA. {saber.jafarpour, bullo}@engineering.ucsb.edu

Unfortunately, none of the techniques mentioned above can be extended for characterizing frequency synchronization of Kuramoto model with general topology and arbitrary weights. The early works [24, §VII(A)] [11, Theorem 2.1] present necessary conditions for synchronization. As of today, the sharpest known necessary conditions are given by [3] and are associated to the cutsets of the graph. Beside these necessary conditions, numerous different sufficient conditions have also been derived in the literature. The intuition behind most of these conditions is that the Kuramoto model achieves frequency synchronization when the couplings between the oscillators dominate the dissimilarities in the natural frequencies. An ingenious approach based on graph theoretic ideas is proposed in [24]: if 2-norm of the natural frequencies of the oscillators is bounded by some connectivity measure of the graph, then the network achieves a locally stable frequency synchronization [24, Theorem 2]. Other 2-norm conditions have been derived in the literature using quadratic Lyapunov function [11, Theorem 4.2] [14, Theorem 4.4] and sinusoidal Lyapunov function [19, Proposition 1]. To the best of our knowledge, the tightest 2-norm sufficient condition for existence of stable synchronization manifolds for general topologies is given by [13, Theorem 4.7]. Moreover, using numerical simulation on random graphs and IEEE test cases, it is shown that the necessary and sufficient condition for synchronization of acyclic graph can be considered as a good approximation for frequency synchronization of a large class of graphs [17]. Despite all these deep and fundamental works, up to date, the gap between the necessary and sufficient conditions for frequency synchronization of Kuramoto model is in general huge and the problem of finding accurate and provably correct synchronization conditions is far from resolved. Finally, we mention that, parallel to the above analytical results, a large body of literature in synchronization is devoted to the numerical analysis of synchronization for specific random graphs such as small-world and scale free networks [6], [35], [34]. We refer the interested readers to [1], [16], [5] for survey of available results on frequency synchronization and region of attraction of the synchronized manifold as well as to [38], [44], [30] for examples of recent developments and engineering applications.

*c) Contributions:* As preliminary contributions, first, for a given weighted undirected graph  $G$ , we introduce the cutset projection matrix of  $G$ , as the oblique projection onto the cutset space of  $G$  parallel to the weighted cycle space of  $G$ . We find a compact matrix form for the cutset projection of  $G$  in terms of incidence matrix and Laplacian matrix of  $G$  and study its properties, including its  $\infty$ -norm for acyclic, unweighted complete graphs and unweighted ring graphs. Secondly, for a given graph  $G$  and angle  $\gamma \in [0, \pi)$ , we introduce the embedded cohesive subset  $S^G(\gamma)$  on the  $n$ -torus. This subset is larger than the arc subset, but smaller than the cohesive subset studied in [14], [16]. We present an explicit algorithm for checking whether an element of the  $n$ -torus is in  $S^G(\gamma)$  or not. We show that, for a network of Kuramoto oscillators, achieving locally exponentially stable frequency synchronization and existence of a synchronization manifold are equivalent in the domain  $S^G(\gamma)$ , for every  $\gamma \in [0, \pi/2]$ .

Our main contribution is a new family of sufficient conditions for the existence of synchronized solutions to a network of Kuramoto oscillators. We start by using the cutset projection operator to rewrite the Kuramoto equilibrium equation in an equivalent edge balance form. Our first and main set of sufficient conditions for synchronization is obtained via a concise proof that exploits this edge balance form and the Brouwer Fixed-Point Theorem. These conditions require the norm of the edge flow quantity  $B^T L^\dagger \omega$  to be smaller than a critical threshold; here  $L$  is the graph Laplacian and  $B$  is the (oriented) incidence matrix. This first main set of conditions have various advantages and one disadvantage. The first advantage is that the conditions apply to any graph topology, edge weights, and natural frequencies. The second advantage is that the conditions are stated with respect to an arbitrary norm; in other words, one can select or design a preferable norm to express the condition in. Finally, our conditions bring clarity to a conjecture arising in [17]: while focusing on separated connectivity and heterogeneity measures results in overly-conservative estimates of the synchronization threshold, using combined measures leads to tighter estimates. Building on the work in [17], our novel approach establishes the role of the combined connectivity and heterogeneity measure  $B^T L^\dagger \omega$  and results in sharper synchronization estimates.

The disadvantage of our first main set of conditions is that the critical threshold is equal to the minimum amplification factor of a scaled projection operator, that is, to the solution of a nonconvex minimization problem. Instead of focusing on this minimization problem, we here contribute two explicit lower bounds on the critical threshold and two corresponding sufficient conditions for synchronization. First, when  $p = 2$  and the graph is unweighted, we present an explicit lower bound on the critical threshold which leads to a sharper synchronization test than the best previously-known 2-norm test in the literature. Second, we present a general lower bound on the critical threshold which leads to a family of explicit  $p$ -norm tests for synchronization. For  $p \neq 2$ , these  $p$ -norm tests are the first rigorous conditions of their kind. In particular, for  $p = \infty$ , the  $\infty$ -norm test establishes rigorously a modified version of the approximate test proposed in [17]. Specifically, while the test proposed in [17] was already shown to be inaccurate for certain counterexamples, our  $\infty$ -norm test here is a correct, more-conservative, and generically-applicable version of it.

One additional advantage of this work is that our unifying technical approach is based on a single concise proof method, from which various special cases are obtained as corollaries. In particular, we show that our sufficient conditions are: equal to those in the literature for acyclic graphs, sharper than those in the literature for unweighted ring graphs, and slightly more conservative than those in the literature for unweighted complete graphs. Finally, we apply our  $\infty$ -norm test to a class of IEEE test cases from the MATPOWER package [47]. We measure a test accuracy as a percentage of the numerically-computed exact threshold. For IEEE test cases with number of nodes in the approximate range 100–2500, we show how our test improves the accuracy of the sufficient synchronization condition from 0.11%–0.29% to 23.08%–43.70%.

*d) Paper organization:* In Section II, we review the Kuramoto model. In Section III, we present some preliminary results, including the cutset projection operator. Section IV contains this paper's main results the new family of  $p$ -norm synchronization tests. Finally, Section IV-B is devoted to a comparative analysis of the new sufficient conditions.

*e) Notation:* For  $n \in \mathbb{N}$ , let  $\mathbf{1}_n$  (resp.  $\mathbf{0}_n$ ) denote the vector in  $\mathbb{R}^n$  with all entries equal to 1 (resp. 0), and define the vector subspace  $\mathbf{1}_n^\perp = \{x \in \mathbb{R}^n \mid \mathbf{1}_n^\top x = 0\}$ . For  $n \in \mathbb{N}$ , the  $n$ -torus and  $n$ -sphere are denoted by  $\mathbb{T}^n$  and  $\mathbb{S}^n$ , respectively. Given two points  $\alpha, \beta \in \mathbb{S}^1$ , the clockwise arc-length between  $\alpha$  and  $\beta$  and the counterclockwise arc-length between  $\alpha$  and  $\beta$  are denoted by  $\text{dist}_c(\alpha, \beta)$  and  $\text{dist}_{cc}(\alpha, \beta)$  respectively. The geodesic distance between  $\alpha$  and  $\beta$  in  $\mathbb{S}^1$  is defined by

$$|\alpha - \beta| = \min\{\text{dist}_c(\alpha, \beta), \text{dist}_{cc}(\alpha, \beta)\}. \quad (1)$$

For  $z \in \mathbb{C}$ , the real and imaginary part of  $z$  are denoted by  $\Re(z)$  and  $\Im(z)$ , respectively. For  $x \in \mathbb{R}^n$  and  $p \in [1, \infty)$ , the  $p$ -norm of  $x$  is  $\|x\|_p = \sqrt[p]{|x_1|^p + \dots + |x_n|^p}$  and the  $\infty$ -norm of  $x$  is  $\|x\|_\infty = \max\{|x_i| \mid i \in \{1, \dots, n\}\}$ . For  $A \in \mathbb{R}^{n \times m}$ , the  $p$ -norm of  $A$  is  $\|A\|_p = \max\{\|Ax\|_p \mid \|x\|_p = 1\}$ . We let  $A^\top$  denote the transpose of  $A$ . The eigenvalues of a symmetric matrix  $A \in \mathbb{R}^{n \times n}$  are real and denoted by  $\lambda_1(A) \leq \dots \leq \lambda_n(A)$ . For symmetric matrices  $A, B \in \mathbb{R}^{n \times n}$ , we write  $A \preceq B$  if  $B - A$  is positive semidefinite. The Moore–Penrose pseudoinverse of  $A \in \mathbb{R}^{n \times m}$  is the unique  $A^\dagger \in \mathbb{R}^{m \times n}$  satisfying  $AA^\dagger A = A$ ,  $A^\dagger AA^\dagger = A^\dagger$ ,  $(AA^\dagger)^\top = AA^\dagger$ , and  $(A^\dagger A)^\top = A^\dagger A$ . Given a set  $S \subseteq \mathbb{R}^m$  and matrix  $A \in \mathbb{R}^{n \times m}$ , we define the set  $AS \subseteq \mathbb{R}^n$  by  $AS = \{A\mathbf{v} \mid \mathbf{v} \in S\}$ . Given subspaces  $S$  and  $T$  of  $\mathbb{R}^n$ , the *minimal angle* between  $S$  and  $T$  is  $\arccos(\max\{x^\top y \mid x \in S, y \in T, \|x\|_2 = \|y\|_2 = 1\})$ .

If the vector spaces  $S$  and  $T$  satisfy  $S \oplus T = \mathbb{R}^n$ , then, for every  $x \in \mathbb{R}^n$ , there exist unique  $x_S \in S$  and  $x_T \in T$  such that  $x = x_S + x_T$ ; the vector  $x_S$  is called the *oblique projection* of  $x$  onto  $S$  parallel to  $T$  and the map  $\mathcal{P} : \mathbb{R}^n \rightarrow S$  defined by  $\mathcal{P}(x) = x_S$  is the *oblique projection operator* onto  $S$  parallel to  $T$ . If  $T = S^\perp$ , then  $\mathcal{P}$  is the *orthogonal projection* onto  $S$ .

An undirected weighted graph is a triple  $G = (V, \mathcal{E}, A)$ , where  $V$  is the set of vertices with  $|V| = n$ ,  $\mathcal{E} \subseteq V \times V$  is the set of edges with  $|\mathcal{E}| = m$ , and  $A = A^\top \in \mathbb{R}^{n \times n}$  is the nonnegative adjacency matrix. The Laplacian  $L \in \mathbb{R}^{n \times n}$  of  $G$  is defined by  $L = \text{diag}\left(\left\{\sum_{j \in V} a_{ij}\right\}_{i \in V}\right) - A$ . A path in  $G$  is an ordered sequence of vertices such that there is an edge between every two consecutive vertices. A path is *simple* if no vertex appears more than once in it, except possibly for the case when the initial and final vertices are the same. A *cycle* is a simple path that starts and ends at the same vertex and has at least three vertices. If the graph  $G$  is connected, then  $\dim(\text{Im}(L)) = n - 1$  [21, Lemma 13.1.1]. After choosing an enumeration and orientation for the edges of  $G$ , we let  $B \in \mathbb{R}^{n \times m}$  denote the oriented incidence matrix of  $G$ . For a connected  $G$ , we have  $\text{Im}(B) = \mathbf{1}_n^\perp$ . It is known that  $BAB^\top = L$ , where  $A \in \mathbb{R}^{m \times m}$  is the diagonal weight matrix defined by  $A_{ef} = a_{ij}$  if both edges  $e$  and  $f$  are equal to  $(i, j)$ , and 0 otherwise. For every vector  $\mathbf{v} \in \mathbb{R}^m$ , we define  $L_{\mathbf{v}} \in \mathbb{R}^{n \times n}$  by  $L_{\mathbf{v}} = BA \text{diag}(\mathbf{v})B^\top$ .

## II. THE KURAMOTO MODEL

The Kuramoto model is a system of  $n$  oscillators, where each oscillator has a natural frequency  $\omega_i \in \mathbb{R}$  and is described by a phase angle  $\theta_i \in \mathbb{S}^1$ . The interconnection of the oscillators is described by a weighted undirected connected graph  $G = (\{1, \dots, n\}, \mathcal{E}, A)$ , with nodes  $\{1, \dots, n\}$ , edges  $\mathcal{E} \subseteq \{1, \dots, n\} \times \{1, \dots, n\}$ , and weights  $a_{ij} = a_{ji} > 0$ . The dynamics for the Kuramoto model is:

$$\dot{\theta}_i = \omega_i - \sum_{j=1}^n a_{ij} \sin(\theta_i - \theta_j), \quad \text{for } i \in \{1, \dots, n\}. \quad (2)$$

In matrix language, using the incidence matrix  $B$  associated to an arbitrary orientation of the graph and the weight matrix  $A$ , one can write the differential equations (2) as:

$$\dot{\theta} = \omega - BA \sin(B^\top \theta), \quad (3)$$

where  $\theta = (\theta_1, \theta_2, \dots, \theta_n)^\top \in \mathbb{T}^n$  is the phase vector and  $\omega = (\omega_1, \omega_2, \dots, \omega_n)^\top \in \mathbb{R}^n$  is the natural frequency vector. For every  $s \in [0, 2\pi)$ , the clockwise rotation of  $\theta \in \mathbb{T}^n$  by the angle  $s$  is the function  $\text{rot}_s : \mathbb{T}^n \rightarrow \mathbb{T}^n$  defined by

$$\text{rot}_s(\theta) = (\theta_1 + s, \theta_2 + s, \dots, \theta_n + s)^\top, \quad \text{for } \theta \in \mathbb{T}^n.$$

Given  $\theta \in \mathbb{T}^n$ , define the equivalence class  $[\theta]$  by

$$[\theta] = \{\text{rot}_s(\theta) \mid s \in [0, 2\pi)\}.$$

The quotient space of  $\mathbb{T}^n$  under the above equivalence class is denoted by  $\mathbb{T}^n / \text{rot}$ . If  $\theta : \mathbb{R}_{\geq 0} \rightarrow \mathbb{T}^n$  is a solution for the Kuramoto model (3) then, for every  $s \in [0, 2\pi)$ , the curve  $\text{rot}_s(\theta) : \mathbb{R}_{\geq 0} \rightarrow \mathbb{T}^n$  is also a solution of (3). Therefore, for the rest of this paper, we consider the state space of the Kuramoto model (3) to be  $\mathbb{T}^n / \text{rot}$ .

**Definition 1 (Frequency synchronization).** (i) A solution  $\theta : \mathbb{R}_{\geq 0} \rightarrow \mathbb{T}^n$  of the Kuramoto model (3) achieves frequency synchronization if there exists a synchronous frequency function  $\omega_{\text{syn}} : \mathbb{R}_{\geq 0} \rightarrow \mathbb{R}$  such that

$$\lim_{t \rightarrow \infty} \dot{\theta}(t) = \omega_{\text{syn}}(t) \mathbf{1}_n.$$

(ii) For a subset  $S$  of the torus  $\mathbb{T}^n$ , the coupled oscillator (3) achieves frequency synchronization if, for every  $\theta_0 \in S$ , the trajectory of (3) starting at  $\theta_0$  achieves frequency synchronization.

If a solution of the coupled oscillator (3) achieves frequency synchronization, then by summing all the equations in (3) and taking the limit as  $t \rightarrow \infty$ , we obtain  $\omega_{\text{syn}} = \sum_{i=1}^n \omega_i / n$ . Therefore, the synchronous frequency is constant and is equal to the average of the natural frequency of the oscillators. By choosing a rotating frame with the frequency  $\frac{\omega_{\text{syn}}}{n}$ , one can assume that  $\omega \in \mathbf{1}_n^\perp$ .

**Definition 2 (Synchronization manifold).** Let  $\theta^*$  be a solution of the algebraic equation

$$\omega = BA \sin(B^\top \theta^*). \quad (4)$$

Then  $[\theta^*]$  is a synchronization manifold for the Kuramoto model (3).

In other words, the synchronization manifolds of the Kuramoto model (3) are the equilibrium manifolds of the differential equations (3).

**Theorem 3 (Characterization of frequency synchronization).** *Consider the Kuramoto model (3), with the graph  $G$ , incidence matrix  $B$ , weight matrix  $A$ , and natural frequencies  $\omega \in \mathbb{1}_n^\perp$ . Then the following statements are equivalent:*

- (i) *there exists an open set  $U \subset \mathbb{T}^n$  such that every solution of the Kuramoto model (3) achieves frequency synchronization;*
- (ii) *there exists a locally asymptotically stable synchronization manifold for (3).*

### III. PRELIMINARY RESULTS

#### A. The cutset projection associated to a weighted digraph

We here introduce and study a useful oblique projection operator; to the best of our knowledge, this operator and its graph theoretic interpretation have not been studied previously. We start with some definitions for a digraph  $G$  with  $n$  nodes and  $m$  edges. For a simple path  $\gamma$  in  $G$ , we define the *signed weighted path vector*  $v^\gamma \in \mathbb{R}^m$  of the simple path  $\gamma$  by

$$v_e^\gamma = \begin{cases} +1/a_{kl}, & \text{if the edge } e = (k, l) \text{ is traversed positively by } \gamma, \\ -1/a_{kl}, & \text{if the edge } e = (k, l) \text{ is traversed negatively by } \gamma, \\ 0, & \text{otherwise.} \end{cases}$$

For a partition of the vertices of  $V$  in two non-empty disjoint sets  $\phi$  and  $\phi^c$ , the *cutset orientation vector* corresponding to the partition  $V = \phi \cup \phi^c$  is the vector  $v^\phi \in \mathbb{R}^m$  given by

$$v_e^\phi = \begin{cases} +1, & \text{if edge } e \text{ has its source node in } \phi \\ & \text{and its sink node in } \phi^c, \\ -1, & \text{if edge } e \text{ has its source node in } \phi^c \\ & \text{and its sink node in } \phi, \\ 0, & \text{otherwise.} \end{cases}$$

The *weighted cycle space* of  $G$  is the subspace of  $\mathbb{R}^m$  spanned by the signed weighted path vectors of all simple undirected cycles in  $G$ . (Note that the notion of cycle space is standard, while that of weighted cycle space is not.) The *cutset space* of  $G$  is subspace of  $\mathbb{R}^m$  spanned by the cutset orientation vectors of all cuts of the nodes of  $G$ . It is a variation of a known fact, e.g., see [9, Theorem 8.5], that

weighted cycle space

$$= \text{span}\{v^\gamma \in \mathbb{R}^m \mid \gamma \text{ is a simple cycle in } G\} = \text{Ker}(BA),$$

cutset space

$$= \text{span}\{v^\phi \in \mathbb{R}^m \mid \phi \text{ is a cut of } G\} = \text{Img}(B^\top).$$

**Theorem 4 (Decomposition of edge space and the cutset projection).** *Let  $G$  be an undirected weighted connected graph with  $n$  nodes and  $m$  edges, incidence matrix  $B$ , and weight matrix  $A$ . Recall that the Laplacian of  $G$  is given by  $L = BAB^\top$ . Then*

- (i) *the edge space  $\mathbb{R}^m$  can be decomposed as the direct sum:*

$$\mathbb{R}^m = \text{Img}(B^\top) \oplus \text{Ker}(BA);$$

- (ii) *the cutset projection matrix  $\mathcal{P}$ , defined to be the oblique projection onto  $\text{Img}(B^\top)$  parallel to  $\text{Ker}(BA)$ , is given by*

$$\mathcal{P} = B^\top L^\dagger BA; \quad (5)$$

- (iii) *the cutset projection matrix  $\mathcal{P}$  is idempotent, and 0 and 1 are eigenvalues with algebraic (and geometric) multiplicity  $m - n + 1$  and  $n - 1$ , respectively.*

The proof of this theorem is given in Appendix A. Recall that, given a full rank matrix  $C$ , the orthogonal projection onto  $\text{Img}(C)$  is given by the formula  $C(C^\top C)^{-1}C^\top$ . As we show in Appendix A, the equality (5) is an application of a generalized version of this formula. Next, we establish some properties of the cutset projection matrix, whose proof is again postponed to Appendix A.

**Theorem 5 (Properties of the cutset projection).** *Consider an undirected weighted connected graph  $G$  with incidence matrix  $B$ , weight matrix  $A$ , and cutset projection matrix  $\mathcal{P}$ . Then the following statements hold:*

- (i) *if  $G$  is unweighted (that is,  $A = I_m$ ), then  $\mathcal{P}$  is an orthogonal projection matrix and  $\|\mathcal{P}\|_2 = 1$ ;*
- (ii) *if  $G$  is acyclic, then  $\mathcal{P} = I_m$  and  $\|\mathcal{P}\|_\infty = 1$ ;*
- (iii) *if  $G$  is an unweighted complete graph, then  $\mathcal{P} = \frac{1}{n}B^\top B$  and  $\|\mathcal{P}\|_\infty = \frac{2(n-1)}{n}$ ; and*
- (iv) *if  $G$  is an unweighted ring graph, then  $\mathcal{P} = I_n - \frac{1}{n}\mathbb{1}_n\mathbb{1}_n^\top$  and  $\|\mathcal{P}\|_\infty = \frac{2(n-1)}{n}$ .*

We conclude with some observations without proof.

**Remark 6** (Connection with effective resistances and minimal angle). *With the same notation as in Theorem 5,*

- (i) *the decomposition  $\mathbb{R}^m = \text{Img}(B^\top) \oplus \text{Ker}(BA)$  and the cutset projection matrix  $\mathcal{P}$  depend on the edge orientation chosen on  $G$ . However, it can be shown that, for every  $p \in [1, \infty) \cup \{\infty\}$ , the induced norm  $\|\mathcal{P}\|_p$  is independent of the specific orientation;*
- (ii) *if  $R_{\text{eff}} \in \mathbb{R}^{n \times n}$  is the matrix of effective resistances of the weighted graph  $G$ , then  $\mathcal{P} = -\frac{1}{2}B^\top R_{\text{eff}}BA$  [20]; and*
- (iii) *if  $\theta$  is the minimal angle between the cutset space of  $G$  and the weighted cycle space of  $G$ , then  $\sin(\theta) = \|\mathcal{P}\|_2^{-1}$  [23, Theorem 3.1].*

#### B. Embedded cohesive subset

In this subsection, we introduce a new subset of the  $n$ -torus, called the embedded cohesive subset. This subset plays an essential role in our analysis of the Kuramoto model (3). In what follows, recall that  $|\theta_i - \theta_j|$  is the geodesic distance on  $\mathbb{T}$  between angles  $\theta_i$  and  $\theta_j$ , as defined in equation (1).

**Definition 7 (Arc subset, cohesive subset, and embedded cohesive subsets).** *Let  $G$  be an undirected weighted connected graph with edge set  $\mathcal{E}$  and let  $\gamma \in [0, \pi)$ .*

- (i) *The arc subset  $\bar{\Gamma}(\gamma) \subset \mathbb{T}^n$  is the set of  $\theta \in \mathbb{T}^n$  such that there exists an arc of length  $\gamma$  in  $\mathbb{S}^1$  containing all angles  $\theta_1, \theta_2, \dots, \theta_n$ . The set  $\Gamma(\gamma)$  is the interior of  $\bar{\Gamma}(\gamma)$ ;*

(ii) The cohesive subset  $\Delta^G(\gamma) \subseteq \mathbb{T}^n$  is

$$\Delta^G(\gamma) = \{\theta \in \mathbb{T}^n \mid |\theta_i - \theta_j| \leq \gamma, \text{ for all } (i, j) \in \mathcal{E}\};$$

(iii) The embedded cohesive subset  $S^G(\gamma) \subseteq \mathbb{T}^n$  is

$$S^G(\gamma) = \{\text{rot}_s(\exp(i\mathbf{x})) \mid \mathbf{x} \in B^G(\gamma) \text{ and } s \in [0, 2\pi)\},$$

where we define  $B^G(\gamma) = \{\mathbf{x} \in \mathbb{1}_n^\perp \mid \|B^\top \mathbf{x}\|_\infty \leq \gamma\}$ .

It is easy to see that the arc subsets, the cohesive subsets, and the embedded cohesive subset are invariant under the rotations  $\text{rot}_s$ , for every  $s \in [0, 2\pi)$ . Therefore, in the rest of this paper, without any ambiguity, we use the notations  $\Gamma(\gamma)$ ,  $\Delta^G(\gamma)$ , and  $S^G(\gamma)$  for the set of equivalent classes of the arc subsets, the cohesive subset, and the embedded cohesive subset, respectively.

Note that it is clear how to check whether a point in  $\mathbb{T}^n$  belongs to the arc subset and/or the cohesive subset. We next present an algorithm, called the Embedding Algorithm, that allows one to easily check whether a point in  $\mathbb{T}^n$  belongs to the embedded cohesive set or not.

---

### Embedding Algorithm

---

**Input:**  $\theta \in \mathbb{T}^n$

```

1:  $x_1 := 0$  and  $S := \{1\}$ 
2: while  $|S| < n$  :
3:   pick  $\{j, k\} \in \mathcal{E}$  s.t.  $j \in S$  and  $k \in \{1, \dots, n\} \setminus S$ 
4:   if geodesic arc from  $\theta_j$  to  $\theta_k$  is counterclockwise :
5:      $x_k := x_j + |\theta_j - \theta_k|$ 
6:   else
7:      $x_k := x_j - |\theta_j - \theta_k|$ 
8:    $S := S \cup \{k\}$ 
9:  $\mathbf{x}_i^\theta := x_i - \text{average}(x_1, \dots, x_n)$  for  $i \in \{1, \dots, n\}$ 
10: return  $\mathbf{x}^\theta \in \mathbb{1}_n^\perp$ 

```

---

We now characterize the embedded cohesive set; the proof of the following theorem is given in Appendix B.

**Theorem 8 (Characterization of the embedded cohesive subset).** *Let  $G$  be an undirected weighted connected graph and  $\gamma \in [0, \pi)$ . For  $\theta \in \mathbb{T}^n$ , let  $\mathbf{x}^\theta \in \mathbb{1}_n^\perp$  be the corresponding output of the Embedding Algorithm. Then the following statements holds:*

- (i)  $\bar{\Gamma}(\gamma) \subseteq S^G(\gamma) \subseteq \Delta^G(\gamma)$ ;
- (ii)  $\exp(i\mathbf{x}^\theta) \in [\theta]$ ;
- (iii)  $[\theta] \in S^G(\gamma)$  if and only if  $\mathbf{x}^\theta \in B^G(\gamma)$ ; and
- (iv) the set  $S^G(\gamma)$  is diffeomorphic with  $B^G(\gamma)$  and the set  $S^G(\gamma)$  is compact.

Based on Theorem 8(iv), in the rest of this paper, we identify the embedded cohesive subset  $S^G(\gamma)$  by the set  $B^G(\gamma) = \{\mathbf{x} \in \mathbb{1}_n^\perp \mid \|B^\top \mathbf{x}\|_\infty \leq \gamma\}$ . We conclude this subsection with an instructive comparison.

**Example 9 (Comparing the three subsets).** *Pick  $\gamma \in [0, \pi)$ . In this example, we show that each of the inclusions in Theorem 8(i) is strict in general.*

- (i) Consider a 5-cycle graph  $G_1$  with the vector  $\theta = (0 \quad \frac{2\pi}{5} \quad \frac{4\pi}{5} \quad \frac{6\pi}{5} \quad \frac{8\pi}{5})^\top$  as shown in Figure 1. One can

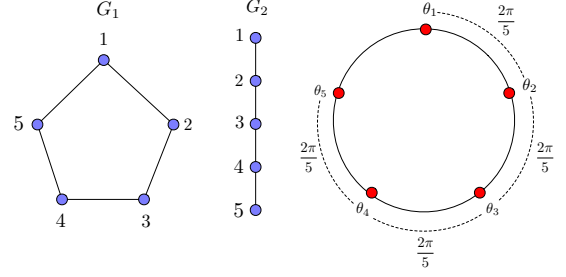


Fig. 1: For the graph  $G_1$ , the 5-tuple defined by the red points on the circle belongs to the cohesive subset  $\Delta^{G_1}(\frac{2\pi}{5})$  but it does not belong to the embedded cohesive subset  $S^{G_1}(\frac{2\pi}{5})$ . For the graph  $G_2$ , this 5-tuple belongs to the embedded cohesive subset  $S^{G_2}(\frac{2\pi}{5})$  but it does not belong to the arc subset  $\bar{\Gamma}(\frac{2\pi}{5})$ .

verify that  $|\theta_i - \theta_j| = \frac{2\pi}{5}$ , for every  $(i, j) \in \mathcal{E}$  and therefore  $\theta \in \Delta^{G_1}(\gamma)$ . However, using the embedding algorithm, it can be shown that  $\theta \notin S^{G_1}(\frac{2\pi}{5})$ .

- (ii) Consider an acyclic graph  $G_2$  with 5 nodes and the vector  $\theta = (0 \quad \frac{2\pi}{5} \quad \frac{4\pi}{5} \quad \frac{6\pi}{5} \quad \frac{8\pi}{5})^\top$  as shown in Figure 1. Then it is clear that  $\theta \notin \bar{\Gamma}(\frac{2\pi}{5})$ . However, using the embedding algorithm, it can be shown that  $\theta \in S^{G_2}(\frac{2\pi}{5})$ .

### C. Kuramoto map and its properties

We now define the Kuramoto map  $f_K : \mathbb{1}_n^\perp \rightarrow \text{Im}(B^\top)$  by

$$f_K(\mathbf{x}) = \mathcal{P} \sin(B^\top \mathbf{x}). \quad (6)$$

This map arises naturally from the Kuramoto model as follows. Recall that, given nodal variables  $\omega \in \mathbb{1}_n^\perp \subset \mathbb{R}^n$  and given the identification in Theorem 8(iv), the equilibrium equation (4) can be rewritten as

$$\omega = B\mathcal{A} \sin(B^\top \mathbf{x}) \quad (7)$$

and can be interpreted as a nodal balance equation. If one left-multiplies this nodal balance equation by  $B^\top L^\dagger$ , then one obtains an edge balance equation

$$B^\top L^\dagger \omega = \mathcal{P} \sin(B^\top \mathbf{x}) = f_K(\mathbf{x}), \quad (8)$$

where  $B^\top L^\dagger \omega \in \text{Im}(B^\top) \subset \mathbb{R}^m$  can be interpreted as a collection of flows through each edge.

The following theorem studies the properties of the map  $f_K$  and shows the equivalence between the nodal and edge balance equations; see Appendix C for the proof.

**Theorem 10 (Basic properties of the Kuramoto map).** *Consider the Kuramoto model (3), with the graph  $G$ , incidence matrix  $B$ , weight matrix  $\mathcal{A}$ , and natural frequencies  $\omega \in \mathbb{1}_n^\perp$ . Define the Kuramoto map as in (6) and pick  $\gamma \in [0, \frac{\pi}{2})$ . Then the following statements hold:*

- (i)  $\mathbf{x}^*$  is a synchronization manifold for the Kuramoto model (3) if and only if  $\mathbf{x}^*$  solves the nodal balance equation (7) if and only if  $\mathbf{x}^*$  solves edge nodal balance equation (8);
- (ii) the function  $f_K$  is real analytic and one-to-one on  $S^G(\gamma)$ ;
- (iii) if there exists a synchronization manifold  $\mathbf{x}^* \in S^G(\gamma)$ , then it is unique and locally exponentially stable.

#### IV. SUFFICIENT CONDITIONS FOR SYNCHRONIZATION

In this section, we present novel sufficient conditions for existence and uniqueness of the synchronization manifold for the Kuramoto model in the domain  $S^G(\gamma)$ , for  $\gamma \in [0, \frac{\pi}{2})$ . We start with a useful definition.

**Definition 11 (Minimum amplification factor for scaled projection).** Consider an undirected weighted connected graph with incidence matrix  $B$ , weight matrix  $\mathcal{A}$ , and cutset projection matrix  $\mathcal{P}$ . For  $\gamma \in [0, \frac{\pi}{2})$  and  $p \in [1, \infty) \cup \{\infty\}$ , define

- (i) the domain  $D_p(\gamma) = \{\mathbf{y} \in \mathbb{R}^m \mid \|\mathbf{y}\|_p \leq \gamma\} \cap \text{Img}(B^\top)$ ;
- (ii) for  $\mathbf{y} \in D_p(\gamma)$ , the scaled cutset projection operator  $\mathcal{P} \text{diag}(\text{sinc}(\mathbf{y})) : \text{Img}(B^\top) \rightarrow \text{Img}(B^\top)$ ; and
- (iii) the minimum amplification factor of the scaled cutset projection  $\mathcal{P} \text{diag}(\text{sinc}(\mathbf{y}))$  on  $D_p(\gamma)$  by:

$$\alpha_p(\gamma) = \min_{\mathbf{y} \in D_p(\gamma)} \min_{\substack{\mathbf{z} \in \text{Img}(B^\top) \\ \|\mathbf{z}\|_p = 1}} \|\mathcal{P} \text{diag}(\text{sinc}(\mathbf{y})) \mathbf{z}\|_p.$$

Note that  $\alpha_p(\gamma)$  is well-defined because  $(\mathbf{y}, \mathbf{z}) \mapsto \mathcal{P} \text{diag}(\text{sinc}(\mathbf{y})) \mathbf{z}$  is a continuous function over a compact set. The proof of the following lemma is given in Appendix D.

**Lemma 12 (The minimum amplification factor is non-zero).** With the same notation and under the same assumptions as Definition 11, the minimum amplification factor of the scaled projection satisfies  $\alpha_p(\gamma) > 0$ .

##### A. Main results

Now, we are ready to state the main results of this paper. We start with a family of general conditions for synchronization of Kuramoto model (3).

**Theorem 13 (General sufficient conditions for synchronization).** Consider the Kuramoto model (3) with undirected weighted connected graph  $G$ , the incidence matrix  $B$ , the weight matrix  $\mathcal{A}$ , the cutset projection  $\mathcal{P}$ , and frequencies  $\omega \in \mathbb{1}_n^\perp$ . For  $\gamma \in [0, \frac{\pi}{2})$ , if there exists  $p \in [1, \infty) \cup \{\infty\}$  such that

$$\|B^\top L^\dagger \omega\|_p \leq \alpha_p(\gamma) \gamma, \quad (\text{T1})$$

then there exists a unique locally exponentially stable synchronization manifold  $\mathbf{x}^*$  for the Kuramoto model (3) in the domain  $S^G(\gamma)$ .

Note that one can generalize test (T1) to the setting of arbitrary sub-multiplicative norms, with the caveat that the solution may take value outside  $S^G(\gamma)$ .

*Proof of Theorem 13.* We first show that, for every  $p \in [1, \infty) \cup \{\infty\}$ , we have  $D_p(\gamma) \subseteq B^\top(S^G(\gamma))$ . Suppose that  $\mathbf{y} \in D_p(\gamma)$ . Then, by definition of  $D_p(\gamma)$ , there exists  $\xi \in \mathbb{1}_n^\perp$  such that  $\mathbf{y} = B^\top \xi$  and  $\|B^\top \xi\|_p \leq \gamma$ . Note that, for any vector  $y$ , the  $p$ -norm of  $y$  is larger than or equal to the  $\infty$ -norm of  $y$ . This implies that  $\|B^\top \xi\|_\infty \leq \|B^\top \xi\|_p \leq \gamma$ . Therefore, by definition of  $S^G(\gamma)$ , we obtain  $\xi \in S^G(\gamma)$  and, as a result, we have  $\mathbf{y} = B^\top \xi \in B^\top(S^G(\gamma))$ . Suppose that  $\gamma \in [0, \frac{\pi}{2})$

and  $\mathbf{x} \in S^G(\gamma)$ . Then  $\mathbf{x}$  is a synchronization manifold for the Kuramoto model (3) if and only if

$$\mathcal{P} \text{diag}(\text{sinc}(B^\top \mathbf{x})) B^\top \mathbf{x} = B^\top L^\dagger \omega.$$

For every  $\mathbf{y} \in D_p(\gamma)$ , define the map  $Q(\mathbf{y}) : \text{Img}(B^\top) \rightarrow \text{Img}(B^\top)$  by

$$Q(\mathbf{y})(\mathbf{z}) = \mathcal{P} \text{diag}(\text{sinc}(\mathbf{y})) \mathbf{z}.$$

The following lemma, whose proof is given in Appendix E, studies some of the properties of the map  $Q(\mathbf{y})$ .

**Lemma 14.** For every  $\mathbf{y} \in D_p(\gamma)$ , then the map  $Q(\mathbf{y})$  is invertible and, for every  $\mathbf{z} \in \text{Img}(B^\top)$ ,

$$(Q(\mathbf{y}))^{-1} \mathbf{z} = (B^\top L_{\text{sinc}(\mathbf{y})}^\dagger B \mathcal{A}) \mathbf{z}. \quad (9)$$

Now we get back to the proof of Theorem 13. For every  $p \in [1, \infty) \cup \{\infty\}$  and every  $\gamma \in [0, \frac{\pi}{2})$  define the map  $h_p : D_p(\gamma) \rightarrow \text{Img}(B^\top)$  by

$$h_p(\mathbf{y}) = (Q(\mathbf{y}))^{-1} (B^\top L^\dagger \omega).$$

Note that by Lemma 14, we have

$$h_p(\mathbf{y}) = (B^\top L_{\text{sinc}(\mathbf{y})}^\dagger B \mathcal{A})(B^\top L^\dagger \omega) = B^\top L_{\text{sinc}(\mathbf{y})}^\dagger \omega.$$

For every  $\mathbf{y} \in D_p(\gamma)$ , we have  $\dim(\text{Img}(L_{\text{sinc}(\mathbf{y})})) = n - 1$ . Therefore, by [37, Theorem 4.2], the map  $h_p$  is continuous on  $D_p(\gamma)$ . We first show that, if the assumption (T1) holds, then  $h_p(\gamma) \subseteq D_p(\gamma)$ . Given  $\omega \in \mathbb{1}_n^\perp$ , note the following inequality:

$$\begin{aligned} \|h_p(\mathbf{y})\|_p &= \|(Q(\mathbf{y}))^{-1} (B^\top L^\dagger \omega)\|_p \\ &\leq \max_{\mathbf{y} \in D_p(\gamma)} \|(Q(\mathbf{y}))^{-1}\|_p \|B^\top L^\dagger \omega\|_p. \end{aligned} \quad (10)$$

Since  $Q(\mathbf{y})$  is invertible, using Lemma 24 in Appendix D,

$$\begin{aligned} \max_{\mathbf{y} \in D_p(\gamma)} \|(Q(\mathbf{y}))^{-1}\|_p &= \left( \min_{\mathbf{y} \in D_p(\gamma)} \min_{\substack{\mathbf{z} \in \text{Img}(B^\top) \\ \|\mathbf{z}\|_p = 1}} \|Q(\mathbf{y}) \mathbf{z}\|_p \right)^{-1} \\ &= \frac{1}{\alpha_p(\gamma)}. \end{aligned} \quad (11)$$

Combining the inequalities (10), (11), and (T1), we obtain

$$\|h_p(\mathbf{y})\|_p \leq \frac{1}{\alpha_p(\gamma)} \|B^\top L^\dagger \omega\|_p \leq \frac{1}{\alpha_p(\gamma)} \alpha_p(\gamma) \gamma \leq \gamma.$$

In summary,  $h_p$  is a continuous map from a compact convex set into itself. Therefore, by the Brouwer Fixed-Point Theorem,  $h_p$  has a fixed-point in  $D_p(\gamma)$ . Since, for every  $p \in [1, \infty) \cup \{\infty\}$ , we have  $D_p(\gamma) \subseteq B^\top(S^G(\gamma))$ , there exists  $\mathbf{x} \in S^G(\gamma)$  such that  $h_p(B^\top \mathbf{x}) = B^\top \mathbf{x}$ . Therefore, we have

$$B^\top L^\dagger \omega = \mathcal{P} \text{diag}(\text{sinc}(B^\top \mathbf{x})).$$

The fact that  $\mathbf{x}$  is the unique synchronization manifold of the Kuramoto model (3) in  $S^G(\gamma)$  follows from Theorem 10 parts (i) and (iii).  $\square$

Theorem 13 presents a novel family of sufficient synchronization conditions for the Kuramoto model (3). However, these tests require the computation of the minimum amplification factor  $\alpha_p(\gamma)$ , that is, the solution to an optimization problem (see Definition 11) that is generally nonconvex. At this time we do not know of any reliable numerical method to

compute  $\alpha_p(\gamma)$  for large dimensional systems. Therefore, in what follows, we focus on finding explicit lower bounds on  $\alpha_p(\gamma)$ , thereby obtaining computable synchronization tests.

**Theorem 15 (Sufficient conditions for synchronization based on 2-norm).** *Consider the Kuramoto model (3) with undirected unweighted connected graph  $G$ , the incidence matrix  $B$ , the cutset projection matrix  $\mathcal{P}$ , and frequencies  $\omega \in \mathbb{1}_n^\perp$ . Then the following statements hold:*

(i) for every  $\gamma \in [0, \frac{\pi}{2})$ ,

$$\alpha_2(\gamma) \geq \text{sinc}(\gamma);$$

(ii) for every  $\gamma \in [0, \frac{\pi}{2})$ , if the following condition holds:

$$\|B^\top L^\dagger \omega\|_2 \leq \sin(\gamma), \quad (\text{T2})$$

then there exists a unique locally exponentially stable synchronization manifold  $\mathbf{x}^*$  for the Kuramoto model (3) in the domain  $S^G(\gamma)$ .

*Proof.* First note that  $\text{diag}(\text{sinc}(\mathbf{x})) \succeq \text{sinc}(\gamma)I_m$ , for every  $\mathbf{x} \in D_2(\gamma)$ . This implies that

$$L_{\text{sinc}(\mathbf{x})} = B \text{diag}(\text{sinc}(\mathbf{x})) B^\top \succeq \text{sinc}(\gamma)L. \quad (12)$$

Multiplying both sides of the inequality (12) by  $(L^\dagger)^{\frac{1}{2}}$ , we get

$$(L^\dagger)^{\frac{1}{2}} L_{\text{sinc}(\mathbf{x})} (L^\dagger)^{\frac{1}{2}} \succeq \text{sinc}(\gamma) (I_n - \frac{1}{n} \mathbb{1}_n \mathbb{1}_n^\top).$$

Note that  $\lambda_i(I_n - \frac{1}{n} \mathbb{1}_n \mathbb{1}_n^\top) = 1$ , for every  $i \in \{2, \dots, n\}$ . Thus, [22, Corollary 7.7.4 (c)] implies

$$\lambda_i((L^\dagger)^{\frac{1}{2}} L_{\text{sinc}(\mathbf{x})} (L^\dagger)^{\frac{1}{2}}) \geq \text{sinc}(\gamma), \quad i \in \{2, \dots, n\}.$$

In turn this inequality implies

$$\lambda_i(L^{\frac{1}{2}} L_{\text{sinc}(\mathbf{x})}^\dagger L^{\frac{1}{2}}) \leq \frac{1}{\text{sinc}(\gamma)}, \quad i \in \{2, \dots, n\}.$$

Now, Weyl's Theorem [22, Theorem 4.3.1] implies

$$\frac{1}{\text{sinc}(\gamma)} (I_n - \frac{1}{n} \mathbb{1}_n \mathbb{1}_n^\top) \succeq L^{\frac{1}{2}} L_{\text{sinc}(\mathbf{x})}^\dagger L^{\frac{1}{2}},$$

so that, for every  $\mathbf{x} \in D_2(\gamma)$ ,

$$L^\dagger \succeq \text{sinc}(\gamma) L_{\text{sinc}(\mathbf{x})}^\dagger. \quad (13)$$

Regarding part (i), note that  $\mathcal{P} = B^\top L^\dagger B$  is an idempotent symmetric matrix. Thus, by setting  $\mathbf{y} = B^\top \mathbf{w}$ , we have

$$\begin{aligned} & \|\mathcal{P} \text{diag}(\text{sinc}(\mathbf{x})) \mathbf{y}\|_2^2 \\ &= \mathbf{w}^\top B \text{diag}(\text{sinc}(\mathbf{x})) B^\top L^\dagger B \text{diag}(\text{sinc}(\mathbf{x})) B^\top \mathbf{w}. \end{aligned}$$

Therefore, using (12) and (13), we get

$$\begin{aligned} & \|\mathcal{P} \text{diag}(\text{sinc}(\mathbf{x})) \mathbf{y}\|_2^2 \\ &= \mathbf{w}^\top B \text{diag}(\text{sinc}(\mathbf{x})) B^\top L^\dagger B \text{diag}(\text{sinc}(\mathbf{x})) B^\top \mathbf{w} \\ &\geq \text{sinc}(\gamma) \mathbf{w}^\top B \text{diag}(\text{sinc}(\mathbf{x})) B^\top \mathbf{w} \\ &\geq \text{sinc}(\gamma)^2 \mathbf{w}^\top B B^\top \mathbf{w} = \text{sinc}(\gamma)^2 \mathbf{y}^\top \mathbf{y} = \text{sinc}(\gamma)^2. \end{aligned}$$

This completes the proof of part (i). Regarding part (ii), if the assumption (T2) holds, then

$$\|B^\top L^\dagger \omega\|_2 \leq \sin(\gamma) = \text{sinc}(\gamma)\gamma \leq \alpha_2(\gamma)\gamma.$$

The result follows by using the test (T1) for  $p = 2$ .  $\square$

It is now convenient to introduce the smooth function  $g : [1, \infty) \rightarrow \mathbb{R}$  defined by

$$g(x) = \frac{y(x) + \sin(y(x))}{2} - x \frac{y(x) - \sin(y(x))}{2} \Big|_{y(x) = \arccos(\frac{x-1}{x+1})}, \quad (14)$$

One can verify that  $g(1) = 1$ ,  $g$  is monotonically decreasing, and  $\lim_{x \rightarrow \infty} g(x) = 0$ ; the graph of  $g$  is shown in Figure 2.

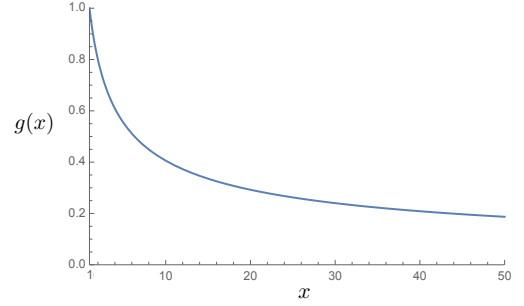


Fig. 2: The graph of the monotonically-decreasing function  $g$

**Theorem 16 (Sufficient conditions for synchronization based on general lower bound).** *Consider the Kuramoto model (3) with undirected weighted connected graph  $G$ , the incidence matrix  $B$ , the weight matrix  $\mathcal{A}$ , the cutset projection matrix  $\mathcal{P}$ , and frequencies  $\omega \in \mathbb{1}_n^\perp$ . For  $p \in [1, \infty) \cup \{\infty\}$ , define the angle*

$$\gamma_p^* = \arccos\left(\frac{\|\mathcal{P}\|_p - 1}{\|\mathcal{P}\|_p + 1}\right) \in [0, \frac{\pi}{2}). \quad (15)$$

Then the following statements hold:

(i) for every  $\gamma \in [0, \frac{\pi}{2})$ , we have

$$\alpha_p(\gamma) \geq \left(\frac{1 + \text{sinc}(\gamma)}{2}\right) - \|\mathcal{P}\|_p \left(\frac{1 - \text{sinc}(\gamma)}{2}\right);$$

(ii) if the following condition holds:

$$\|B^\top L^\dagger \omega\|_p \leq g(\|\mathcal{P}\|_p), \quad (\text{T3})$$

then there exists a unique locally exponentially stable synchronization manifold  $\mathbf{x}^*$  for the Kuramoto model (3) in the domain  $S^G(\gamma_p^*)$ .

*Proof.* Regarding part (i), let  $\mathbf{w} \in \mathbb{R}^m$ . The triangle inequality implies that, for every  $\mathbf{y} \in D_p(\gamma)$  and every  $\mathbf{z} \in \text{Im}(B^\top)$  with  $\|\mathbf{z}\|_p = 1$ ,

$$\begin{aligned} & \|\mathcal{P} \text{diag}(\text{sinc}(\mathbf{y})) \mathbf{z}\|_p \\ &\geq \|\mathcal{P} \text{diag}(\mathbf{w}) \mathbf{z}\|_p - \|\mathcal{P} \text{diag}(\text{sinc}(\mathbf{y}) - \mathbf{w}) \mathbf{z}\|_p. \end{aligned} \quad (16)$$

Using triangle inequality, the last term in the inequality (16) can be upper bounded as

$$\|\mathcal{P} \text{diag}(\text{sinc}(\mathbf{y}) - \mathbf{w}) \mathbf{z}\|_p \leq \|\mathcal{P}\|_p \|\text{diag}(\text{sinc}(\mathbf{y}) - \mathbf{w})\|_p,$$

Moreover, the matrix  $\text{diag}(\text{sinc}(\mathbf{y}) - \mathbf{w})$  is diagonal and by [22, Theorem 5.6.36], we have

$$\|\text{diag}(\text{sinc}(\mathbf{y}) - \mathbf{w})\|_p = \|\text{sinc}(\mathbf{y}) - \mathbf{w}\|_\infty.$$

Therefore, the inequality (16) can be rewritten as

$$\begin{aligned} & \|\mathcal{P} \text{diag}(\text{sinc}(\mathbf{y}))\mathbf{z}\|_p \\ & \geq \|\mathcal{P} \text{diag}(\mathbf{w})\mathbf{z}\|_p - \|\mathcal{P}\|_p \|\text{sinc}(\mathbf{y}) - \mathbf{w}\|_\infty. \end{aligned}$$

By setting  $\mathbf{w} = \left(\frac{1+\text{sinc}(\gamma)}{2}\right) \mathbf{1}_m$ , we have

$$\|\mathcal{P} \text{diag}(\mathbf{w})\mathbf{z}\|_p = \left(\frac{1+\text{sinc}(\gamma)}{2}\right) \|\mathcal{P}\mathbf{z}\|_p = \frac{1+\text{sinc}(\gamma)}{2}.$$

In turn  $\|\text{sinc}(\mathbf{y}) - \mathbf{w}\|_\infty \leq \frac{1-\text{sinc}(\gamma)}{2}$ , and we get

$$\begin{aligned} & \|\mathcal{P} \text{diag}(\text{sinc}(\mathbf{y}))\mathbf{z}\|_p \\ & \geq \left(\frac{1+\text{sinc}(\gamma)}{2}\right) - \|\mathcal{P}\|_p \left(\frac{1-\text{sinc}(\gamma)}{2}\right). \end{aligned}$$

Part (i) of the theorem simply follows by taking the minimum over  $\mathbf{y} \in D_p(\gamma)$  and  $\mathbf{z} \in \text{Img}(B^\top)$  such that  $\|\mathbf{z}\|_p = 1$ .

Regarding part (ii), note that, by part (i), we have

$$\alpha_p(\gamma) \geq \left(\frac{\gamma + \sin(\gamma)}{2}\right) - \|\mathcal{P}\|_p \left(\frac{\gamma - \sin(\gamma)}{2}\right).$$

Define the function  $\ell : [0, \frac{\pi}{2}] \rightarrow \mathbb{R}$  by

$$\ell(\gamma) = \left(\frac{\gamma + \sin(\gamma)}{2}\right) - \|\mathcal{P}\|_p \left(\frac{\gamma - \sin(\gamma)}{2}\right).$$

Then one can compute:

$$\frac{d\ell}{d\gamma}(\gamma) = \left(\frac{1 + \cos(\gamma)}{2}\right) - \|\mathcal{P}\|_p \left(\frac{1 - \cos(\gamma)}{2}\right), \quad (17)$$

$$\frac{d^2\ell}{d\gamma^2}(\gamma) = \left(\frac{-\sin(\gamma)}{2}\right) - \|\mathcal{P}\|_p \left(\frac{\sin(\gamma)}{2}\right). \quad (18)$$

Using the equation (17), one can check that the unique critical point of  $\ell$  in the interval  $[0, \frac{\pi}{2}]$  is the solution  $\gamma_p^*$  to

$$\left(\frac{1 + \cos(\gamma_p^*)}{2}\right) - \|\mathcal{P}\|_p \left(\frac{1 - \cos(\gamma_p^*)}{2}\right) = 0.$$

This implies that  $\gamma_p^* \in [0, \frac{\pi}{2})$  is given as in equation (15). Moreover, we have

$$\frac{d^2\ell}{d\gamma^2}(\gamma_p^*) = \left(\frac{-\sin(\gamma_p^*)}{2}\right) - \|\mathcal{P}\|_p \left(\frac{\sin(\gamma_p^*)}{2}\right) < 0,$$

so that  $\gamma = \gamma_p^*$  is a local maximum for  $\ell$ . Now by using test (T1), if the following condition holds:

$$\|B^\top L^\dagger \omega\|_p \leq \alpha_p(\gamma_p^*) \gamma_p^*,$$

then there exists a unique locally exponentially stable synchronization manifold  $\mathbf{x}^*$  for the Kuramoto model (3) in the domain  $S^G(\gamma_p^*)$ . Using the lower bound for  $\alpha_p(\gamma)$  given in part (i), it is easy to see that if the following condition holds:

$$\begin{aligned} \|B^\top L^\dagger \omega\|_p & \leq \left(\frac{\gamma_p^* + \sin(\gamma_p^*)}{2}\right) - \|\mathcal{P}\|_p \left(\frac{\gamma_p^* - \sin(\gamma_p^*)}{2}\right) \\ & = g(\|\mathcal{P}\|_p), \end{aligned}$$

then there exists a unique locally exponentially stable synchronization manifold  $\mathbf{x}^*$  for the Kuramoto model (3) in the domain  $S^G(\gamma_p^*)$ . This completes the proof of the theorem.  $\square$

**Remark 17** (Comparison of test (T2) and test (T3)). (i)

The tests (T2) and (T3) have different domain of applicability. For every  $\gamma \in [0, \frac{\pi}{2})$ , the test (T2) presents a sufficient condition for synchronization of the Kuramoto model (3) in  $S^G(\gamma)$ . Instead, the test (T3) is applicable only to the specific domain  $S^G(\gamma_p^*)$  for  $\gamma_p^* = \arccos\left(\frac{\|\mathcal{P}\|_p - 1}{\|\mathcal{P}\|_p + 1}\right) \in [0, \frac{\pi}{2})$ .

(ii) For unweighted graphs with  $\gamma = \frac{\pi}{2}$ , one can recover test (T2) from test (T3). Specifically, for unweighted graphs, Theorem 5(i) implies that  $\gamma_2^* = \arccos(0) = \frac{\pi}{2}$ . Thus, for unweighted graphs, test (T3) with  $p = 2$  is  $\|B^\top L^\dagger \omega\|_2 \leq g(1) = \sin(\frac{\pi}{2}) = 1$ .

## B. Comparison with previously-known synchronization results

We now compare the new synchronization tests (T2) and (T3) with those existing in the literature.

### 1) General topology (2-norm synchronization conditions):

To the best of our knowledge, sufficient conditions for synchronization of networks of oscillators with general topology was first studied in the paper [24]. Using the analysis methods introduced in [24], the tightest sufficient condition for synchronization of networks of oscillators with general topology [13, Theorem 4.7] can be obtained by the following test:

$$\|B^\top \omega\|_2 < \lambda_2(L), \quad (T0)$$

where  $\lambda_2(L)$  is the Fiedler eigenvalue of the Laplacian  $L$  (see the survey [16] for more discussion). One can show that, for unweighted graphs test (T2) gives a sharper sufficient condition than test (T0). This fact is a consequence of the following lemma, whose proof is given in Appendix F.

**Lemma 18.** Let  $G$  be a connected, undirected, weighted graph with the incidence matrix  $B$  and weight matrix  $\mathcal{A}$ . Assume that  $L$  is the Laplacian of  $G$  with eigenvalues  $0 = \lambda_1(L) < \lambda_2(L) \leq \dots \leq \lambda_n(L)$ . Then the following statements hold:

(i) each  $\omega \in \mathbb{1}_n^\perp$  satisfies the inequality

$$\|B^\top L^\dagger \omega\|_2 \leq \frac{1}{\lambda_2(L)} \|B^\top \omega\|_2, \quad (19)$$

with the equality sign if and only if  $\omega$  belongs to the eigenspace associated to  $\lambda_2(L)$ ; and

(ii) if  $\omega \in \mathbb{1}_n^\perp$  satisfies test (T0), then it satisfies test (T2).

### 2) General topology ( $\infty$ -norm synchronization conditions):

The approximate test  $\|B^\top L^\dagger \omega\|_\infty \leq 1$  was proposed in [17] as an approximately-correct sufficient condition for synchronization; statistical evidence on random graphs and IEEE test cases shows that the condition has much predictive power. However, [17] also identifies a family of counterexamples, where the condition is shown to be incorrect. Our test (T3) with  $p = \infty$  is a rigorous, more conservative, and generically-applicable version of that approximately-correct test.

3) *Acyclic topology:* Consider the Kuramoto model (3) with acyclic connected graph  $G$  and  $\omega \in \mathbb{1}_n^\perp$ . Then the existence and uniqueness of synchronization manifolds of (3) in  $S^G(\gamma)$  can be completely characterized by the following test [16, Corollary 7.5]:

$$\|B^\top L^\dagger \omega\|_\infty \leq \sin(\gamma). \quad (20)$$

We show that this characterization can be obtained from the general test (T1) for  $p = \infty$ .

**Corollary 19 (Synchronization for acyclic graphs).** *Consider the Kuramoto model (3) with the acyclic undirected weighted connected graph  $G$ , the incidence matrix  $B$ , the weight matrix  $A$ , and  $\omega \in \mathbb{1}_n^\perp$ . Pick  $\gamma \in [0, \frac{\pi}{2})$ . Then the following conditions are equivalent:*

- (i)  $\|B^T L^\dagger \omega\|_\infty \leq \sin(\gamma)$ ,
- (ii) *there exists a unique locally exponentially stable synchronization manifold for the Kuramoto model (3) in  $S^G(\gamma)$ .*

*Additionally, if either of the above equivalent conditions holds, then the unique synchronization manifold in  $S^G(\gamma)$  is  $L^\dagger B A \arcsin(B^T L^\dagger \omega)$ .*

*Proof.* Since  $G$  is acyclic, Theorem 5(ii) implies that  $\mathcal{P} = B^T L^\dagger B A = I_m = I_{n-1}$ .

(i)  $\implies$  (ii): Note that, for every  $\mathbf{y} \in D_\infty(\gamma)$  and every  $\mathbf{z} \in \text{Img}(B^T)$  such that  $\|\mathbf{z}\|_\infty = 1$ , we have

$$\|\text{diag}(\text{sinc}(\mathbf{y}))\mathbf{z}\|_\infty \geq \text{sinc}(\gamma)\|\mathbf{z}\|_\infty = \text{sinc}(\gamma).$$

In turn, this implies that

$$\begin{aligned} \alpha_\infty(\gamma) &= \min_{\mathbf{y} \in D_\infty(\gamma)} \min_{\substack{\mathbf{z} \in \text{Img}(B^T), \\ \|\mathbf{z}\|_\infty = 1}} \|\mathcal{P} \text{diag}(\text{sinc}(\mathbf{y}))\mathbf{z}\|_\infty \\ &= \min_{\mathbf{y} \in D_\infty(\gamma)} \min_{\substack{\mathbf{z} \in \text{Img}(B^T), \\ \|\mathbf{z}\|_\infty = 1}} \|\text{diag}(\text{sinc}(\mathbf{y}))\mathbf{z}\|_\infty \\ &= \text{sinc}(\gamma). \end{aligned}$$

Therefore, by using the test (T1) for  $p = \infty$ , there exists a unique locally stable synchronization manifold for the Kuramoto model (3).

(ii)  $\implies$  (i): If there exists a unique locally stable synchronization manifold  $\mathbf{x}^*$  for the Kuramoto model (3) in  $S^G(\gamma)$ , by Theorem 10(i), we have

$$B^T L^\dagger \omega = \mathcal{P} \sin(B^T \mathbf{x}^*) = \sin(B^T \mathbf{x}^*).$$

Since  $\mathbf{x}^* \in S^G(\gamma)$  and  $\gamma \in [0, \frac{\pi}{2})$ , we have  $\|\sin(B^T \mathbf{x}^*)\|_\infty \leq \sin(\gamma)$  and, in turn,

$$\|B^T L^\dagger \omega\|_\infty \leq \sin(\gamma).$$

This completes the proof of equivalence of (i) and (ii). If  $\mathbf{x}^*$  is a synchronization manifold for the Kuramoto model (3) in  $S^G(\gamma)$ , then we have  $B^T L^\dagger \omega = \mathcal{P} \sin(B^T \mathbf{x}^*) = \sin(B^T \mathbf{x}^*)$ . This implies that

$$B^T \mathbf{x}^* = \arcsin(B^T L^\dagger \omega).$$

Therefore, by pre-multiplying both side of the above equality into  $BA$ , we obtain

$$BAB^T \mathbf{x}^* = L \mathbf{x}^* = BA \arcsin(B^T L^\dagger \omega).$$

Thus, since  $\mathbf{x}^* \in \mathbb{1}_n^\perp$ , we get  $\mathbf{x}^* = L^\dagger BA \arcsin(B^T L^\dagger \omega)$ . This completes the proof of the theorem.  $\square$

**Remark 20** (Alternative way to recover acyclic case). *One can prove Corollary 19, using the lower bounds given in Theorem 16(i). Note that, for acyclic graphs, Theorems 5(ii) and 16(i) imply that  $\alpha_\infty(\gamma) \geq \text{sinc}(\gamma)$ . Combining this bound with the test (T1) for  $p = \infty$ , we obtain  $\|B^T L^\dagger \omega\|_\infty \leq \sin(\gamma)$ .*

4) *Unweighted ring graphs and unweighted complete graphs:* To the best of our knowledge, the sharpest sufficient condition for existence of a synchronization manifold in the domain  $S^G(\gamma)$  for the Kuramoto model (3) with unweighted complete graph  $G$  is given by the following test [16, Theorem 6.6]:

$$\|B^T L^\dagger \omega\|_\infty \leq \sin(\gamma), \quad (21)$$

and for the Kuramoto model (3) with unweighted ring graph  $G$  is given by the following test [17, Theorem 3, Condition 3]:

$$\|B^T L^\dagger \omega\|_\infty \leq \frac{1}{2} \sin(\gamma). \quad (22)$$

One can use the lower bound given in Theorem 16(i) to obtain another sufficient conditions for synchronization of unweighted complete and ring graphs.

**Corollary 21 (Sufficient synchronization conditions for unweighted complete and ring graphs).** *Consider the Kuramoto model (3) with either unweighted complete or unweighted ring graph  $G$ , the incidence matrix  $B$ , cutset projection  $\mathcal{P}$ , and  $\omega \in \mathbb{1}_n^\perp$ . For every  $n \in \mathbb{N}$ , define the scalar function  $h_n : [0, \frac{\pi}{2}) \rightarrow \mathbb{R}_{\geq 0}$  by*

$$h_n(\gamma) = \sin(\gamma) - \frac{n-2}{2n}(\gamma - \sin(\gamma)). \quad (23)$$

*If the following condition holds:*

$$\|B^T L^\dagger \omega\|_\infty \leq h_n(\gamma),$$

*then there exists a unique locally stable synchronization manifold  $\mathbf{x}^*$  for the Kuramoto model (3) in  $S^G(\gamma)$*

*Proof.* By Theorem 5(iii) and (iv), the  $\infty$ -norm of the cutset projection matrix  $\mathcal{P}$  for graph  $G$  with  $n$  nodes which is either unweighted complete or unweighted ring, is given by  $\|\mathcal{P}\|_\infty = \frac{2(n-1)}{n}$ . Therefore, Theorem 16(i) implies the following lower bound:

$$\alpha_\infty(\gamma) \geq \text{sinc}(\gamma) - \frac{n-2}{2n}(1 - \text{sinc}(\gamma)). \quad (24)$$

Combining the bound on  $\alpha_\infty(\gamma)$  with the test (T1) for  $p = \infty$ , we get the following test for the synchronization of unweighted complete graphs:

$$\|B^T L^\dagger \omega\|_\infty \leq \sin(\gamma) - \frac{n-2}{2n}(\gamma - \sin(\gamma)) = h_n(\gamma). \quad (25)$$

The proof of the corollary is complete by using Theorem 13.  $\square$

Note that, the function  $\gamma \mapsto (\gamma - \sin(\gamma))$  is positive and increasing on the interval  $\gamma \in (0, \frac{\pi}{2}]$ . Therefore, for every  $k < n$  and every  $\gamma \in [0, \frac{\pi}{2})$ , we have  $h_n(\gamma) \leq h_k(\gamma) \leq \sin(\gamma)$ . Thus, for unweighted complete graphs, the test (25) is more conservative than the existing test (21). It is worth mentioning that the gap between the new test (25) and the existing test (21) decreases with the decrease of the angle  $\gamma$ . For instance, for  $\gamma = \frac{\pi}{2}$ , the right hand side of the test (25) asymptotically converges to  $\frac{3}{2} - \frac{\pi}{2} \approx 0.715 < 1$ . Therefore, at  $\gamma = \frac{\pi}{2}$ , the sufficient test (25) is approximately 28.50 % more conservative than the test (21). Instead, for  $\gamma = \frac{\pi}{4}$ , the

right hand side of the test (25) asymptotically converges to  $\frac{3\sqrt{2}}{4} - \frac{\pi}{8} \approx 0.668 < \sin(\frac{\pi}{4}) = \frac{\sqrt{2}}{2} \approx 0.707$ . This means that, at  $\gamma = \frac{\pi}{4}$ , the test (25) is approximately 5.53 % more conservative than the test (21). The comparison between the graph of the functions  $h_5(x)$ ,  $h_{10}(x)$ , and  $h_{20}(x)$  and  $\sin(x)$  over the interval  $[0, \frac{\pi}{2}]$  is shown in Figure 3.

For unweighted ring graphs, it is easy to see that the sufficient condition (25) is always sharper than the existing sufficient condition (22). The comparison between the graph of the functions  $h_5(x)$ ,  $h_{10}(x)$ , and  $h_{20}(x)$  and  $\frac{1}{2}\sin(x)$  for  $x \in [0, \frac{\pi}{2}]$  is shown in Figure 3.

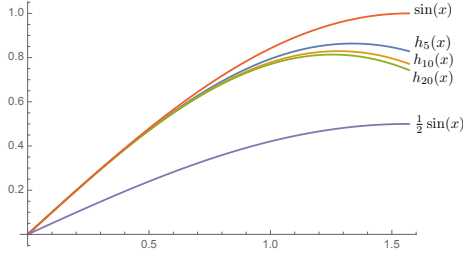


Fig. 3: Comparison of the new sufficient tests with the existing sufficient tests for unweighted complete graphs and unweighted ring graphs.

5) *IEEE test cases:* Here we consider various IEEE test cases described by a connected graph  $G$  and a nodal admittance matrix  $Y \in \mathbb{C}^{n \times n}$ . The set of nodes of  $G$  is partitioned into a set of load buses  $\mathcal{V}_1$  and a set of generator buses  $\mathcal{V}_2$ . The voltage at the node  $j \in \mathcal{V}_1 \cup \mathcal{V}_2$  is denoted by  $V_j$ , where  $V_j = |V_j|e^{i\theta_j}$  and the power demand (resp. power injection) at node  $j \in \mathcal{V}_1$  (resp.  $j \in \mathcal{V}_2$ ) is denoted by  $P_j$ . By ignoring the resistances in the network, the synchronization manifold  $[\theta]$  of the network satisfies the following Kuramoto model [17]:

$$P_j - \sum_{l \in \mathcal{V}_1 \cup \mathcal{V}_2} a_{jl} \sin(\theta_j - \theta_l) = 0, \quad \forall j \in \mathcal{V}_1 \cup \mathcal{V}_2. \quad (26)$$

where  $a_{jl} = a_{lj} = |V_j||V_l|\Im(Y_{jl})$ , for connected nodes  $j$  and  $l$ . For the nine IEEE test cases given in Table I, we numerically check the existence of a synchronization manifold for the Kuramoto model (26) in the domain  $S^G(\pi/2)$ . We consider effective power injections to be a scalar multiplication of nominal power injections, i.e., given nominal injections  $P_j^{\text{nom}}$  we set  $P_j = KP_j^{\text{nom}}$ , for some  $K \in \mathbb{R}_{>0}$  and for every  $j \in \mathcal{V}_1 \cup \mathcal{V}_2$ . The voltage magnitudes at the generator buses are pre-determined and the voltage magnitudes at load buses are computed by solving the reactive power balance equations using the optimal power flow solver provided by MATPOWER [47]. The critical coupling of the Kuramoto model (26) is denoted by  $K_c$  and is computed using MATLAB *fsolve*. For a given test T, the smallest value of scaling factor for which the test T fails is denoted by  $K_T$ . We define the critical ratio of the test T by  $K_T/K_c$ . Intuitively speaking, the critical ratio shows the accuracy of the test T. Table I contains the following information:

**The first two columns** contain the critical ratio of the prior test (T0) from the literature and the new sufficient test (T3) proposed in this paper.

**The third column** gives the critical ratio for the following approximate test proposed in [17]:

$$\|B^T L^\dagger \omega\|_\infty \leq 1. \quad (\text{AT0})$$

**The fourth column** gives the critical ratio for following approximate version of the test (T1):

$$\|B^T L^\dagger \omega\|_\infty \leq (\pi/2)\alpha_\infty^*(\pi/2). \quad (\text{AT1})$$

where  $\alpha_\infty^*(\pi/2)$  is the approximate value for  $\alpha_\infty(\pi/2)$  computed using MATLAB *fmincon*. Test (AT1) is approximate since, in general, *fmincon* may not converge to a solution and, even when it converges, the solution is only guaranteed to be an upper bound for  $\alpha_\infty(\pi/2)$ .

Test Case	Critical ratio $K_T/K_c$			
	$\lambda_2$ test (T0)[13]	$\infty$ -norm test (T3)	Approx. test (AT0) [17]	General test (AT1)
IEEE 9	16.54 %	73.74 %	92.13 %	85.06 % <sup>†</sup>
IEEE 14	8.33 %	59.42 %	83.09 %	81.32 % <sup>†</sup>
IEEE RTS 24	3.86 %	53.44 %	89.48 %	89.48 % <sup>†</sup>
IEEE 30	2.70 %	55.70 %	85.54 %	85.54 % <sup>†</sup>
IEEE 39	2.97 %	67.57 %	100 %	100 % <sup>†</sup>
IEEE 57	0.36 %	40.69 %	84.67 %	—*
IEEE 118	0.29 %	43.70 %	85.95 %	—*
IEEE 300	0.20 %	40.33 %	99.80 %	—*
Polish 2383	0.11 %	29.08 %	82.85 %	—*

<sup>†</sup> *fmincon* has been run for 100 randomized initial phase angles.

\* *fmincon* does not converge.

TABLE I: Comparison of sufficient and approximate synchronizations tests on IEEE test cases in the domain  $S^G(\pi/2)$ .

Note how (i) our ordering  $(T0) < (T3) < (AT0)$  is representative of the tests' accuracy, (ii) our proposed test (T3) is two order of magnitude more accurate than best-known prior test (T0) in the larger test cases, (iii) the two approximate tests (AT0) and (AT1) are comparable (but our proposed test (AT1) is much more computationally complex).

## V. CONCLUSION

In this paper, we introduced and studied the cutset projection, as a geometric operator associated to a weighted undirected graph. This operator naturally appears in the study of networks of Kuramoto oscillators (3); using this operator, we obtained new families of sufficient conditions for network synchronization. For a network of Kuramoto oscillators with incidence matrix  $B$ , Laplacian  $L$  and frequencies  $\omega$ , these sufficient conditions are in the form of upper bounds on the  $p$ -norm of the edge flow quantity  $B^T L^\dagger \omega$ . In other words, our results highlight the important role of this edge flow quantity in the synchronization of Kuramoto oscillators. We show that our results significantly improve the existing sufficient conditions in the literature in general and, specifically, for a number of IEEE power network test cases.

Our approach and results suggest many future research directions. First, it is important to study the cutset projection in more detail and for more special cases. We envision that the cutset projection and its properties will be a valuable tool in the study of network flow systems, above and beyond the case of Kuramoto oscillators. Secondly, it is of interest to

analyze and improve the accuracy of our sufficient conditions. This can be potentially done by designing efficient algorithm for numerical computation (or estimation) of the minimum amplification factor for large graphs. Thirdly, it is interesting to compare our new  $p$ -norm tests, for different  $p \in [0, \infty) \cup \{\infty\}$ , and potentially extend them using more general norms. Finally, in power network applications, it is potentially of significance to generalize our novel approach to study the coupled power flow equations.

#### ACKNOWLEDGMENTS

The authors thank Elizabeth Huang for her helpful comments, and Brian Johnson and Sairaj Dhople for wide-ranging discussions on power networks. The second author would also like to thank Florian Dörfler for countless conversations on Kuramoto oscillators.

#### APPENDIX A

##### PROOF OF THEOREMS 4 AND 5

We report here a useful well-known lemma, which is a simplified version of [7, Theorem 13].

**Lemma 22** (Oblique projections). *For  $m, n \in \mathbb{N}$ , assume the matrices  $X, Y \in \mathbb{R}^{n \times m}$  satisfy  $\text{Img}(X) \oplus \text{Ker}(Y^\top) = \mathbb{R}^n$ . Then the oblique projection matrix onto  $\text{Img}(X)$  parallel to  $\text{Ker}(Y^\top)$  is  $X(Y^\top X)^\dagger Y^\top$ .*

We are now in a position to prove Theorems 4 and 5.

*Proof of Theorem 4.* Regarding the statement (i), we first show that  $\text{Img}(B^\top) \cap \text{Ker}(BA) = \{0_m\}$ . Suppose that  $v \in \text{Img}(B^\top) \cap \text{Ker}(BA)$ . Then there exists  $\xi \in \mathbb{R}^n$  such that  $v = B^\top \xi$  and

$$BAv = BAB^\top \xi = L\xi = 0_n.$$

Since  $G$  is connected, 0 is a simple eigenvalue of the Laplacian  $L$  associated to the eigenvector  $\mathbb{1}_n$ . This implies that  $\xi \in \text{span}\{\mathbb{1}_n\}$  and  $v = B^\top \xi = 0_m$ . Therefore,  $\text{Img}(B^\top) \cap \text{Ker}(BA) = \{0_m\}$ . Moreover, note that:

$$\begin{aligned} \dim(\text{Img}(B^\top)) &= n - 1, \\ \dim(\text{Ker}(BA)) &= \dim(\text{Ker}(B)) = m - \dim(\text{Img}(B)) \\ &= m - n + 1. \end{aligned}$$

Therefore,  $\mathbb{R}^m = \text{Img}(B^\top) \oplus \text{Ker}(BA)$  as in statement (i).

Statement (ii) of the theorem follows directly from Lemma 22 with  $X = B^\top$  and  $Y = AB^\top$ .

Finally, statement (iii) is a known consequence of statements (ii) and (i). It is instructive, anyway, to provide an independent proof. Note the following equalities:

$$\begin{aligned} (B^\top L^\dagger BA) (B^\top L^\dagger BA) &= B^\top L^\dagger (BAB^\top) L^\dagger BA \\ &= B^\top (L^\dagger L) L^\dagger BA. \end{aligned}$$

Using the fact that  $L^\dagger L = LL^\dagger = I_n - \frac{1}{n} \mathbb{1}_n \mathbb{1}_n^\top$ , we obtain  $B^\top L^\dagger L = B^\top$ . This implies that

$$(B^\top L^\dagger BA) (B^\top L^\dagger BA) = B^\top L^\dagger BA.$$

Thus, the cutset projection  $\mathcal{P}$  is an idempotent matrix and its only eigenvalues are 0 and 1 [22, 1.1.P5].  $\square$

*Proof of Theorem 5.* Regarding part (i), when  $\mathcal{A} = I_m$ , we have  $\text{Ker}(BA) = \text{Ker}(B)$ . Moreover, for every  $x \in \text{Img}(B^\top)$ , there exists  $\alpha \in \mathbb{1}_n^\perp$  such that  $B^\top \alpha = x$ . Therefore, for every  $y \in \text{Ker}(B)$ ,

$$x^\top y = (B^\top \alpha)^\top y = \alpha^\top B y = 0.$$

Moreover, we have  $\dim(\text{Img}(B^\top)) + \dim(\text{Ker}(B)) = m$ . This implies that  $\text{Img}(B^\top) = (\text{Ker}(B))^\perp$ . Therefore, the projection  $\mathcal{P} = B^\top L^\dagger B$  is an orthogonal projection.

Regarding part (ii), since  $G$  is acyclic, we have  $|\mathcal{E}| = n - 1$  and  $\text{Img}(B^\top) = \mathbb{R}^{n-1}$ . Now consider a vector  $x \in \mathbb{R}^{n-1}$ . Since  $\text{Img}(B^\top) = \mathbb{R}^{n-1}$ , there exists a unique  $\alpha \in \mathbb{1}_n^\perp$  such that  $x = B^\top \alpha$ . Therefore, we have

$$B^\top L^\dagger BA(x) = B^\top L^\dagger BA(B^\top \alpha) = B^\top L^\dagger L \alpha = B^\top \alpha = x.$$

This implies that  $\mathcal{P} = I_{n-1} = I_m$ .

Regarding part (iii), note that for a unweighted complete graph, we have  $L = n(I_n - \frac{1}{n} \mathbb{1}_n \mathbb{1}_n^\top)$  and  $L^\dagger = \frac{1}{n}(I_n - \frac{1}{n} \mathbb{1}_n \mathbb{1}_n^\top)$  [15, Lemma III.13]. We compute the cutset projection  $\mathcal{P}$  for an unweighted complete graph as follows:

$$\mathcal{P} = B^\top L^\dagger BA = \frac{1}{n} B^\top \left( I_n - \frac{1}{n} \mathbb{1}_n \mathbb{1}_n^\top \right) B (I_m) = \frac{1}{n} B^\top B.$$

Recalling the meaning of the columns of  $B$ , we compute, for any two edges  $e, f \in \mathcal{E}$ ,

$$\mathcal{P}_{ef} = \begin{cases} \frac{2}{n}, & \text{if } e = f, \\ \frac{1}{n}, & \text{if } e \neq f \text{ and } e \text{ and } f \text{ originate or terminate} \\ & \text{at the same node,} \\ -\frac{1}{n}, & \text{if } e \neq f \text{ and } e \text{ originates where } f \text{ terminates} \\ & \text{or vice versa,} \\ 0, & \text{if } e \text{ and } f \text{ have no node in common.} \end{cases}$$

Using this expression, it is easy to see that  $\|\mathcal{P}\|_\infty = \frac{2(n-1)}{n}$ .

Regarding part (iv), first note that, for an unweighted ring graph, one can choose the orientation of  $G$  such that

$$\text{Img}(B^\top) = \mathbb{1}_n^\perp, \quad \text{Ker}(B) = \text{span}\{\mathbb{1}_n\}.$$

Moreover,  $G$  is unweighted and, by part (i), the cutset projection  $\mathcal{P}$  is an orthogonal projection onto  $\text{Img}(B^\top)$ . This implies that  $\mathcal{P} = I_n - \frac{1}{n} \mathbb{1}_n \mathbb{1}_n^\top$  and simple bookkeeping shows that  $\|\mathcal{P}\|_\infty = (1 - 1/n) + (n - 1)/n = 2(n - 1)/n$ .  $\square$

#### APPENDIX B

##### PROOF OF THEOREM 8

We start with a preliminary result.

**Lemma 23.** *Given  $\theta \in \Delta^G(\gamma)$ , let  $\mathbf{x}^\theta = (x_1 \ \dots \ x_n)^\top \in \mathbb{1}_n^\perp$  be the output of the Embedding Algorithm with input  $\theta$ . Then, for every two nodes  $a, b \in \{1, \dots, n\}$ , there exists a simple path  $(i_1, i_2, \dots, i_r)$  in  $G$  such that  $i_1 = a$ ,  $i_r = b$ , and*

$$|x_{i_k} - x_{i_{k-1}}| \leq \gamma, \quad \text{for all } k \in \{2, \dots, r\}.$$

*Proof.* It suffices to show that, for every  $a \in \{2, \dots, n\}$  there exists a simple path  $(1, i_2 \dots i_r)$  from the node 1 to node  $a$  such that, for every  $k$ , we have

$$|x_{i_k} - x_{i_{k-1}}| \leq \gamma.$$

Start with node  $a$ . Suppose that  $a$  is being added to  $S$  in the Embedding algorithm in the  $r$ th iteration. For every  $k \in \{1, \dots, r\}$ , we denote the set  $S$  in the  $k$ th iteration of the Embedding algorithm by  $S_k$ . Therefore  $a \in S_r$  but  $a \notin S_{r-1}$ . Thus, by the algorithm, there exists  $i_{r-1} \in S_{r-1}$  such that  $|x_{i_{r-1}} - x_i| \leq \gamma$ . Now, we can repeat this procedure for  $i_{r-1}$  to get  $i_{r-2}$  such that  $|x_{i_{r-2}} - x_i| \leq \gamma$ . We can continue doing this procedure until we get to the node 1. Thus we get the simple path  $(1, i_1, \dots, i_r = a)$ .  $\square$

We are now ready to provide the main proof of interest.

*Proof of Theorem 8.* Regarding part (i), we first show the inclusion  $S^G(\gamma) \subseteq \Delta^G(\gamma)$ . Let  $\theta \in S^G(\gamma)$ . Then, by definition of  $S^G(\gamma)$ , there exists  $\mathbf{x} \in \mathbb{1}_n^\perp$  and  $s \in [0, 2\pi)$  such that

$$\|B^T \mathbf{x}\|_\infty \leq \gamma, \quad [\theta] = [\exp(i\mathbf{x})].$$

This means that, for every  $(i, j) \in \mathcal{E}$ , we have

$$|\theta_i - \theta_j| = |\exp(ix_i) - \exp(ix_j)| \leq |x_i - x_j| \leq \gamma.$$

Therefore,  $[\theta] \in \Delta^G(\gamma)$ .

Now consider a point  $\theta \in \bar{\Gamma}(\gamma)$ . By definition, there exists an arc of length  $\gamma$  on  $\mathbb{S}^1$  which contains  $\theta_1, \dots, \theta_n$ . Since  $0 \leq \gamma < \pi$ , this implies that there exists  $\mathbf{y} \in \mathbb{R}^n$  such that  $\theta = \exp(i\mathbf{y})$  and, for every  $(i, j) \in \mathcal{E}$ , we have

$$|\theta_i - \theta_j| = |y_i - y_j|.$$

We define the vector  $\mathbf{x} \in \mathbb{1}_n^\perp$  by  $\mathbf{x} = \mathbf{y} - \text{average}(\mathbf{y})\mathbb{1}_n$ . Then it is clear that  $\mathbf{x} \in \mathbb{1}_n^\perp$  and  $[\exp(i\mathbf{x})] = [\exp(i\mathbf{y})] = [\theta]$ . On the other hand, for every  $(i, j) \in \mathcal{E}$ , the distance between  $x_i$  and  $x_j$  is the same as the distance between  $y_i$  and  $y_j$ . Therefore, we have

$$|x_i - x_j| = |y_i - y_j| = |\theta_i - \theta_j| \leq \gamma.$$

This implies that  $\|B^T \mathbf{x}\|_\infty \leq \gamma$ . Therefore,  $\theta \in S^G(\gamma)$ .

Regarding part (ii), using Lemma 23, it is a straightforward exercise to show that if  $\mathbf{x}^\theta = (x_1, \dots, x_n)$ , then we have  $|x_i - x_j| = |\theta_i - \theta_j| + 2\pi k$ , for some  $k \in \mathbb{Z}_{\geq 0}$ . This implies that  $\exp(i\mathbf{x}^\theta) \in [\theta]$ .

Regarding part (iii), suppose that  $\mathbf{x}^\theta \in B^G(\gamma)$ . Then we have  $\|B^T \mathbf{x}^\theta\|_\infty \leq \gamma$ . Since  $[\theta] = [\exp(i\mathbf{x}^\theta)]$ , it is clear that  $[\theta] \in S^G(\gamma)$ .

Now suppose that  $[\theta] \in S^G(\gamma)$ , we will show that  $\mathbf{x}^\theta \in B^G(\gamma)$ . Assume that  $\mathbf{x}^\theta \notin B^G(\gamma)$ . Therefore, there exists  $(a, b) \in \mathcal{E}$  such that  $|x_a - x_b| > \gamma$ . However, by the definition of the set  $S^G(\gamma)$ , there exists  $\mathbf{y} \in \mathbb{1}_n^\perp$  such that  $\theta = [\exp(i\mathbf{y})]$  and  $\|B^T \mathbf{y}\|_\infty \leq \gamma$ . This implies that  $\theta = [\exp(i\mathbf{x})] = [\exp(i\mathbf{y})]$ . Thus, there exists a vector  $\mathbf{v} \in \mathbb{1}_n^\perp$  whose components are integers such that  $\mathbf{y} = \mathbf{x} + 2\pi\mathbf{v}$ . Since we have  $|x_a - x_b| > \gamma$  and  $|y_a - y_b| \leq \gamma$ , we cannot have  $x_a = y_a$  and  $x_b = y_b$ . Therefore,  $v_a \neq 0$  and we have  $y_a = x_a + 2\pi v_a$ . However, by Lemma 23, since  $[\theta] \in S^G(\gamma) \subseteq \Delta^G(\gamma)$ , there exists a simple path  $(i_1, \dots, i_r)$  between the nodes  $a$  and  $b$  such that, for every  $k \in \{1, \dots, r\}$ , we have  $|x_{i_k} - x_{i_{k-1}}| \leq \gamma$ . Since  $|x_a - x_{i_2}| \leq \gamma$  and  $|y_i - y_{i_2}| \leq \gamma$  we have  $y_{i_2} = x_{i_2} + 2\pi v_a$ . Similarly, one can show that  $y_{i_k} = x_{i_k} + 2\pi v_a$ , for every  $k \in \{1, \dots, r\}$ .

This implies that  $y_b = x_b + 2\pi v_a$ . However, this means that  $|x_a - x_b| = |y_a - y_b| \leq \gamma$ , which is a contradiction.

Regarding part (iv), we first show that the set  $B^G(\gamma)$  is compact. Since  $B^G(\gamma) \subset \mathbb{R}^n$ , it suffice to show that it is closed and bounded. We first show that, for every  $\mathbf{x} \in B^G(\gamma)$ , we have

$$-m\pi \leq x_i \leq m\pi, \quad \forall i \in \{1, \dots, n\},$$

where  $m$  is the number of edges. Suppose that  $\mathbf{x} \in B^G(\gamma)$  and for some  $k \in \{1, \dots, n\}$  we have  $x_k > m\pi$ . Since  $\mathbf{x} \in B^G(\gamma)$ , we get

$$|x_i - x_j| \leq \gamma, \quad \forall i, j \in \{1, \dots, n\}.$$

On the other hand,  $\gamma \in [0, \pi)$  and  $G$  is connected. Therefore, for every  $i \in \{1, \dots, n\}$ , there exists a simple path  $(i_1, i_2, \dots, i_r)$  of length at most  $m$  such that  $i_1 = 1$  and  $i_r = k$ . This implies that

$$\begin{aligned} |x_k - x_i| &= |x_k - x_{i_{r-1}} + x_{i_{r-1}} - x_{i_{r-2}} + \dots + x_{i_2} - x_1| \\ &\leq |x_k - x_{i_{r-1}}| + |x_{i_{r-1}} - x_{i_{r-2}}| + \dots + |x_{i_2} - x_1| \\ &\leq m\gamma < m\pi. \end{aligned}$$

Therefore, for every  $i \in \{1, \dots, n\}$ , we have  $x_i > 0$ . As a result, we get  $\mathbb{1}_n^T \mathbf{x} = \sum_{i=1}^n x_i > 0$ , which is a contradiction since  $\mathbf{x} \in B^G(\gamma)$  and we have  $\mathbf{x} \in \mathbb{1}_n^\perp$ . Similarly, one can show that, for every  $\mathbf{x} \in B^G(\gamma)$ , we have  $-m\pi \leq x_i$ , for every  $i \in \{1, \dots, n\}$ . Therefore,  $B^G(\gamma)$  is bounded. The closedness of the set  $B^G(\gamma)$  is clear from continuity of the  $\infty$ -norm. This implies that  $B^G(\gamma)$  is compact. Now we define the map  $\xi : B^G(\gamma) \rightarrow S^G(\gamma)$  by  $\xi(\mathbf{x}) = [\exp(i\mathbf{x})]$ . We show that  $\xi$  is a real analytic diffeomorphism. It is easy to check that, for every  $\mathbf{x} \in B^G(\gamma)$ ,  $D_{\mathbf{x}}\xi$  is an isomorphism. Therefore  $\xi$  is local diffeomorphism for every  $\mathbf{x} \in B^G(\gamma)$ . Now we show that  $\xi$  is one-to-one on the set  $B^G(\gamma)$ . Suppose that, for  $\mathbf{x}, \mathbf{y} \in B^G(\gamma)$ , we have  $\exp(i\mathbf{x}) = \exp(i\mathbf{y})$ . Therefore, we get  $\mathbf{x} = \mathbf{y} + 2\pi\mathbf{v}$ , where  $\mathbf{v} \in \mathbb{1}_n^\perp$  is a vector whose components are integers. We will show that  $\mathbf{v} = \mathbf{0}_n$ . Suppose that  $\mathbf{v} \neq \mathbf{0}_n$ . Since graph  $G$  is connected, there exists  $(i, j) \in \mathcal{E}$  such that  $v_i \neq v_j$ . This implies that

$$x_i - x_j = y_i - y_j + 2\pi(v_i - v_j). \quad (27)$$

Since we have  $\|B^T \mathbf{y}\|_\infty \leq \gamma$ , we get  $|y_i - y_j| \leq \gamma$ . However, by equation (27), we have

$$\begin{aligned} |x_i - x_j| &= |y_i - y_j + 2\pi(v_i - v_j)| \geq 2\pi|v_i - v_j| - |y_i - y_j| \\ &\geq 2\pi - \gamma > \pi. \end{aligned}$$

However, this is a contradiction with the fact that  $\mathbf{x} \in B^G(\gamma)$ . Therefore,  $\mathbf{v} = \mathbf{0}_n$  and the map  $\xi$  is one-to-one. Note that by part (iii),  $\xi$  is also surjective. Therefore, using [29, Corollary 7.10], the map  $\xi$  is a diffeomorphism between  $B^G(\gamma)$  and  $S^G(\gamma)$ . This completes the proof of part (iv).  $\square$

## APPENDIX C PROOF OF THEOREM 10

Regarding part (i), suppose that  $\mathbf{x}^*$  is a synchronization manifold for the Kuramoto model (7). Then  $\omega =$

$BA \sin(B^\top \mathbf{x}^*)$ . By left-multiplying both side of this equation by  $B^\top L^\dagger$ , we get

$$B^\top L^\dagger \omega = B^\top L^\dagger BA \sin(B^\top \mathbf{x}^*) = \mathcal{P} \sin(B^\top \mathbf{x}^*) = f_K(\mathbf{x}^*).$$

On the other hand, suppose that  $\mathbf{x}^*$  satisfies the edge balance equation (8). Then, if we left-multiply both side of this equation by  $BA$ , we get

$$BAB^\top L^\dagger \omega = BA f_K(\mathbf{x}^*) = BA(B^\top L^\dagger BA) \sin(B^\top \mathbf{x}^*)$$

Noting that  $BAB^\top = L$  and  $LL^\dagger = I_n - \frac{1}{n} \mathbb{1}_n \mathbb{1}_n^\top$ , we have

$$(I_n - \frac{1}{n} \mathbb{1}_n \mathbb{1}_n^\top) \omega = (I_n - \frac{1}{n} \mathbb{1}_n \mathbb{1}_n^\top) BA \sin(B^\top \mathbf{x}^*).$$

Moreover, we have  $\mathbb{1}_n^\top B = 0$  and since  $\omega \in \mathbb{1}_n^\perp$ , we get  $\mathbb{1}_n^\top \omega = 0$ . This implies that  $\omega = BA \sin(B^\top \mathbf{x}^*)$ . This completes the proof of part (i).

Regarding part (ii), since the function  $\sin$  is real analytic,  $f_K$  is real analytic. The proof of injectivity of  $f_K$  on the domain  $S^G(\gamma)$  is a straightforward generalization of [4, Corollary 2].

Regarding part (iii), by part (ii) the map  $f_K$  is one-to-one on the domain  $S^G(\gamma)$ . Therefore, if there exists a synchronization manifold  $\mathbf{x}^* \in S^G(\gamma)$ , it is unique. The proof of the fact that  $\mathbf{x}^*$  is locally exponentially stable is given in [17, Lemma 2].

#### APPENDIX D

##### PROOF OF LEMMA 12 AND OF A USEFUL EQUALITY

*Proof of Lemma 12.* By definition of the minimum amplification factor, it is clear that, for every  $\gamma \in [0, \frac{\pi}{2})$  and every  $p \in [1, \infty) \cup \{\infty\}$ , we have  $\alpha_p(\gamma) \geq 0$ . So, to prove the lemma, it suffices to show that, for every  $\gamma \in [0, \frac{\pi}{2})$  and every  $p \in [1, \infty) \cup \{\infty\}$ , we have  $\alpha_p(\gamma) \neq 0$ . Suppose that for some  $\gamma \in [0, \frac{\pi}{2})$  and some  $p \in [1, \infty) \cup \{\infty\}$ , we have  $\alpha_p(\gamma) = 0$ . Since  $D_p(\gamma)$  and  $\{\mathbf{z} \in \text{Img}(B^\top) \mid \|\mathbf{z}\|_p = 1\}$  are compact sets, there exist  $\mathbf{y}_0 \in D_p(\gamma)$  and  $\mathbf{z}_0 \in \text{Img}(B^\top)$  with the property that  $\|\mathbf{z}_0\|_p = 1$  such that

$$\mathcal{P} \text{diag}(\text{sinc}(\mathbf{y}_0)) \mathbf{z}_0 = \mathbf{0}_m.$$

By premultiplying both side of the above equality by  $\mathbf{z}_0^\top \mathcal{A}$ , we get  $\mathbf{z}_0^\top \mathcal{A} \mathcal{P} \text{diag}(\text{sinc}(\mathbf{y}_0)) \mathbf{z}_0 = 0$ . On the other hand, we know

$$\mathbf{z}_0^\top \mathcal{A} \mathcal{P} = \mathbf{z}_0^\top \mathcal{A} B^\top L^\dagger BA = \mathbf{z}_0^\top \mathcal{P}^\top \mathcal{A} = \mathbf{z}_0^\top \mathcal{A},$$

where the last equality is a direct consequence of  $\mathcal{P} \mathbf{z}_0 = \mathbf{z}_0$ . This implies that  $\mathbf{z}_0^\top \mathcal{A} \text{diag}(\text{sinc}(\mathbf{y}_0)) \mathbf{z}_0 = 0$ . Since both  $\mathcal{A}$  and  $\text{diag}(\text{sinc}(\mathbf{y}_0))$  are diagonal positive definite matrices, we have  $\mathbf{z}_0 = \mathbf{0}_m$ . This is a contradiction with the fact that  $\|\mathbf{z}_0\|_p = 1$ .  $\square$

The next result connects the minimum gain of an invertible operator  $T$  with the norm of  $T^{-1}$ .

**Lemma 24.** *Let  $(V, \|\cdot\|_V)$  be a normed real vector space and  $T : V \rightarrow V$  be a bijective linear map. Then*

$$\min\{\|T\mathbf{x}\|_V \mid \|\mathbf{x}\|_V = 1\} = \frac{1}{\|T^{-1}\|_V}.$$

*Proof.* It is well-known and elementary to show that

$$\min\{\|T\mathbf{x}\|_V \mid \|\mathbf{x}\|_V = 1\} = \min\left\{\frac{\|T\mathbf{x}\|_V}{\|\mathbf{x}\|_V} \mid \mathbf{x} \neq \mathbf{0}\right\}. \quad (28)$$

Because the linear map  $T$  is invertible, for every  $\mathbf{x} \in V$  such that  $\mathbf{x} \neq \mathbf{0}$ ,

$$\frac{\|T\mathbf{x}\|_V}{\|\mathbf{x}\|_V} = \frac{1}{\frac{\|\mathbf{x}\|_V}{\|T\mathbf{x}\|_V}} = \frac{1}{\frac{\|T^{-1}\mathbf{y}\|_V}{\|\mathbf{y}\|_V}}, \quad (29)$$

where  $\mathbf{y} = T\mathbf{x}$ . Therefore, by taking the minimum of both side of the equation (29) over  $\mathbf{x} \neq \mathbf{0}$ , we obtain

$$\begin{aligned} \min\left\{\frac{\|T\mathbf{x}\|_V}{\|\mathbf{x}\|_V} \mid \mathbf{x} \neq \mathbf{0}\right\} &= \min\left\{\frac{1}{\frac{\|T^{-1}\mathbf{y}\|_V}{\|\mathbf{y}\|_V}} \mid \mathbf{y} \neq \mathbf{0}\right\} \\ &= \frac{1}{\max\left\{\frac{\|T^{-1}\mathbf{y}\|_V}{\|\mathbf{y}\|_V} \mid \mathbf{y} \neq \mathbf{0}\right\}} = \frac{1}{\|T^{-1}\|_V}. \end{aligned}$$

The result follows by recalling equation (28).  $\square$

#### APPENDIX E

##### PROOF OF LEMMA 14

For every  $\mathbf{y} \in D_p(\gamma)$ , define the linear operator  $T_{\mathbf{y}} : \text{Img}(B^\top) \rightarrow \text{Img}(B^\top)$  by

$$T_{\mathbf{y}}(\mathbf{z}) = B^\top L_{\text{sinc}(\mathbf{y})}^\dagger BA \mathbf{z}.$$

Let  $\mathbf{z} \in \text{Img}(B^\top)$ . Then there exists  $\xi \in \mathbb{1}_n^\perp$  such that  $\mathbf{z} = B^\top \xi$ . This implies that

$$\begin{aligned} Q(\mathbf{y}) \circ T_{\mathbf{y}}(\mathbf{z}) &= Q(\mathbf{y})(B^\top L_{\text{sinc}(\mathbf{y})}^\dagger BA)(B^\top \xi) \\ &= \mathcal{P} \text{diag}(\text{sinc}(\mathbf{y})) (B^\top L_{\text{sinc}(\mathbf{y})}^\dagger L \xi) \\ &= B^\top L^\dagger L_{\text{sinc}(\mathbf{y})} L_{\text{sinc}(\mathbf{y})}^\dagger L \xi. \end{aligned}$$

Since  $\mathbf{y} \in D_p(\gamma)$ , we have  $\dim(\text{Img}(L_{\text{sinc}(\mathbf{y})})) = n - 1$ . This implies that,

$$L_{\text{sinc}(\mathbf{y})}^\dagger L_{\text{sinc}(\mathbf{y})} = L_{\text{sinc}(\mathbf{y})} L_{\text{sinc}(\mathbf{y})}^\dagger = I_n - \frac{1}{n} \mathbb{1}_n \mathbb{1}_n^\top.$$

Therefore, we get

$$Q(\mathbf{y}) \circ T_{\mathbf{y}}(\mathbf{z}) = B^\top L^\dagger L \xi = B^\top \xi = \mathbf{z}.$$

Since both  $Q(\mathbf{y})$  and  $T_{\mathbf{y}}$  are linear operators on  $\text{Img}(B^\top)$ , we deduce that  $Q(\mathbf{y})$  is invertible and, for every  $\mathbf{z} \in \text{Img}(B^\top)$ :

$$(Q(\mathbf{y}))^{-1} \mathbf{z} = T_{\mathbf{y}}(\mathbf{z}) = B^\top L_{\text{sinc}(\mathbf{y})}^\dagger BA \mathbf{z}.$$

This completes the proof of the lemma.

#### APPENDIX F

##### A USEFUL RESULT AND PROOF OF LEMMA 18

Regarding part (i), Note that  $L$  is real and symmetric. Therefore, using singular-value decomposition [22, Corollary 2.6.6], there exists an orthogonal matrix  $U \in \mathbb{R}^{n \times n}$  such that:

$$L = U \text{diag}(0, \lambda_2, \dots, \lambda_n) U^\top,$$

where  $0 < \lambda_2 \leq \dots \leq \lambda_n$  are ordered eigenvalues of  $L$ . Then, using [7, Chapter 6, §2, Corollary 1] the matrix  $L^\dagger$  has the following singular-value decomposition:

$$L^\dagger = U \text{diag}\left(0, \frac{1}{\lambda_2}, \dots, \frac{1}{\lambda_n}\right) U^\top.$$

Since  $\omega \in \mathbb{1}_n^\perp = \text{Im}(B)$ , there exists  $\mathbf{y} \in \mathbb{R}^n$  which satisfies  $\omega = B\mathbf{y}$ . Therefore, we can write

$$\begin{aligned} \|B^\top L^\dagger \omega\|_2^2 &= \left\| B^\top U \text{diag} \left( 0, \frac{1}{\lambda_2}, \dots, \frac{1}{\lambda_n} \right) U^\top B \mathbf{y} \right\|_2^2 \\ &= \mathbf{y}^\top \left( B^\top U \text{diag} \left( 0, \frac{1}{\lambda_2}, \dots, \frac{1}{\lambda_n} \right) U^\top B \right)^2 \mathbf{y}. \end{aligned}$$

Since we have

$$\begin{aligned} \text{diag} \left( 0, \frac{1}{\lambda_2}, \dots, \frac{1}{\lambda_n} \right) &\preceq \text{diag} \left( \frac{1}{\lambda_2}, \frac{1}{\lambda_2}, \dots, \frac{1}{\lambda_2} \right), \\ \mathbf{0} &\preceq B^\top U \text{diag} \left( 0, \frac{1}{\lambda_2}, \dots, \frac{1}{\lambda_n} \right) U^\top B, \end{aligned}$$

we obtain

$$\left( B^\top U \text{diag} \left( 0, \frac{1}{\lambda_2}, \dots, \frac{1}{\lambda_n} \right) U^\top B \right)^2 \preceq \frac{1}{\lambda_2^2} (B^\top U U^\top B)^2.$$

Therefore,

$$\begin{aligned} \|B^\top L^\dagger B \mathbf{y}\|_2^2 &\leq \frac{1}{\lambda_2^2} \mathbf{y}^\top (B^\top U U^\top B)^2 \mathbf{y} \\ &= \frac{1}{\lambda_2^2} \|B^\top U U^\top B \mathbf{y}\|_2^2 = \frac{1}{\lambda_2^2} \|B^\top \omega\|_2^2. \end{aligned} \quad (30)$$

This concludes the proof of inequality. Regarding the equality, suppose that  $i \in \{2, \dots, n\}$  is the smallest positive integer such that  $\lambda_i \neq \lambda_2$ . Note that, by the above analysis, the equality holds for  $\omega = B\mathbf{y} \in \mathbb{1}_n^\perp$  if and only if

$$\|B^\top L^\dagger B \mathbf{y}\|_2^2 = \frac{1}{\lambda_2^2} \mathbf{y}^\top (B^\top U U^\top B)^2 \mathbf{y}. \quad (31)$$

We define the diagonal matrix  $\Lambda$  by

$$\Lambda = \text{diag} \left( \frac{1}{\lambda_2}, \underbrace{0, \dots, 0}_{i-1}, \left( \frac{1}{\lambda_2} - \frac{1}{\lambda_i} \right), \dots, \left( \frac{1}{\lambda_2} - \frac{1}{\lambda_n} \right) \right).$$

This implies that the equality (31) holds if and only if

$$\mathbf{y}^\top B^\top U \Lambda U^\top B^\top \mathbf{y} = 0. \quad (32)$$

Since  $U \Lambda U^\top \succeq 0$ , the equality (32) holds if and only if  $\omega = B^\top \mathbf{y} \in \text{Ker}(U \Lambda U^\top)$ . However, we know that

$$\text{Ker}(U \Lambda U^\top) = \text{span}\{v_2, \dots, v_{i-1}\},$$

where  $v_k$  is the eigenvector associated to the eigenvalue  $\lambda_k$ . This completes the proof of part (i). Regarding part (ii), if  $\omega \in \mathbb{1}_n^\perp$  satisfies test (T0), then we have  $\|B^\top \omega\|_2 < \lambda_2(L)$ . Therefore, by part (i), we have

$$\|B^\top L^\dagger \omega\|_2 \leq \frac{1}{\lambda_2(L)} \|B^\top \omega\|_2 < 1.$$

This means that  $\omega$  satisfies test (T2).

## REFERENCES

- [1] J. A. Acebrón, L. L. Bonilla, C. J. P. Vicente, F. Ritort, and R. Spigler. The Kuramoto model: A simple paradigm for synchronization phenomena. *Reviews of Modern Physics*, 77(1):137–185, 2005. doi:10.1103/RevModPhys.77.137.
- [2] D. Aeyels and J. A. Rogge. Existence of partial entrainment and stability of phase locking behavior of coupled oscillators. *Progress of Theoretical Physics*, 112(6):921–942, 2004. doi:10.1143/PTP.112.921.
- [3] N. Ainsworth and S. Grijalva. A structure-preserving model and sufficient condition for frequency synchronization of lossless droop inverter-based AC networks. *IEEE Transactions on Power Systems*, 28(4):4310–4319, 2013. doi:10.1109/TPWRS.2013.2257887.
- [4] A. Araposthatis, S. Sastry, and P. Varaiya. Analysis of power-flow equation. *International Journal of Electrical Power & Energy Systems*, 3(3):115–126, 1981. doi:10.1016/0142-0615(81)90017-X.
- [5] A. Arenas, A. Díaz-Guilera, J. Kurths, Y. Moreno, and C. Zhou. Synchronization in complex networks. *Physics Reports*, 469(3):93–153, 2008. doi:10.1016/j.physrep.2008.09.002.
- [6] M. Barahona and L. M. Pecora. Synchronization in small-world systems. *Physical Review Letters*, 89:054101, 2002. doi:10.1103/PhysRevLett.89.054101.
- [7] A. Ben-Israel and T. N. E. Greville. *Generalized Inverses: Theory and Applications*. Springer, 2 edition, 2003. doi:10.1007/b97366.
- [8] E. Brown, J. Moehlis, and P. Holmes. On the phase reduction and response dynamics of neural oscillator populations. *Neural Computation*, 16(4):673–715, 2004. doi:10.1162/089976604322860668.
- [9] F. Bullo. *Lectures on Network Systems*. CreateSpace, 1 edition, 2018. With contributions by J. Cortés, F. Dörfler, and S. Martínez. URL: <http://motion.me.ucsb.edu/book-lns>.
- [10] M. C. Chandorkar, D. M. Divan, and R. Adapa. Control of parallel connected inverters in standalone AC supply systems. *IEEE Transactions on Industry Applications*, 29(1):136–143, 1993. doi:10.1109/28.195899.
- [11] N. Chopra and M. W. Spong. On exponential synchronization of Kuramoto oscillators. *IEEE Transactions on Automatic Control*, 54(2):353–357, 2009. doi:10.1109/TAC.2008.2007884.
- [12] F. Dörfler and F. Bullo. On the critical coupling for Kuramoto oscillators. *SIAM Journal on Applied Dynamical Systems*, 10(3):1070–1099, 2011. doi:10.1137/10081530X.
- [13] F. Dörfler and F. Bullo. Exploring synchronization in complex oscillator networks. In *IEEE Conf. on Decision and Control*, pages 7157–7170, Maui, USA, December 2012. doi:10.1109/CDC.2012.6425823.
- [14] F. Dörfler and F. Bullo. Synchronization and transient stability in power networks and non-uniform Kuramoto oscillators. *SIAM Journal on Control and Optimization*, 50(3):1616–1642, 2012. doi:10.1137/110851584.
- [15] F. Dörfler and F. Bullo. Kron reduction of graphs with applications to electrical networks. *IEEE Transactions on Circuits and Systems I: Regular Papers*, 60(1):150–163, 2013. doi:10.1109/TCSI.2012.2215780.
- [16] F. Dörfler and F. Bullo. Synchronization in complex networks of phase oscillators: A survey. *Automatica*, 50(6):1539–1564, 2014. doi:10.1016/j.automatica.2014.04.012.
- [17] F. Dörfler, M. Chertkov, and F. Bullo. Synchronization in complex oscillator networks and smart grids. *Proceedings of the National Academy of Sciences*, 110(6):2005–2010, 2013. doi:10.1073/pnas.1212134110.
- [18] G. B. Ermentrout. Synchronization in a pool of mutually coupled oscillators with random frequencies. *Journal of Mathematical Biology*, 22(1):1–9, 1985. doi:10.1007/BF00276542.
- [19] A. Franci, A. Chaillet, and W. Pasillas-Lépine. Phase-locking between Kuramoto oscillators: Robustness to time-varying natural frequencies. In *IEEE Conf. on Decision and Control*, pages 1587–1592, Atlanta, USA, December 2010. doi:10.1109/CDC.2010.5717876.
- [20] A. Ghosh, S. Boyd, and A. Saberi. Minimizing effective resistance of a graph. *SIAM Review*, 50(1):37–66, 2008. doi:10.1137/050645452.
- [21] C. D. Godsil and G. F. Royle. *Algebraic Graph Theory*. Springer, 2001.
- [22] R. A. Horn and C. R. Johnson. *Matrix Analysis*. Cambridge University Press, 2nd edition, 2012.
- [23] I. C. F. Ipsen and C. D. Meyer. The angle between complementary subspaces. *American Mathematical Monthly*, 102(10):904–911, 1995. doi:10.2307/2975268.
- [24] A. Jadbabaie, N. Motee, and M. Barahona. On the stability of the Kuramoto model of coupled nonlinear oscillators. In *American Control Conference*, pages 4296–4301, Boston, USA, June 2004. doi:10.23919/ACC.2004.1383983.
- [25] G. Jongen, J. Anemüller, D. Bollé, A. C. C. Coolen, and C. Perez-Vicente. Coupled dynamics of fast spins and slow exchange interactions in the XY spin glass. *Journal of Physics A: Mathematical and General*, 34(19):3957–3984, 2001. doi:10.1088/0305-4470/34/19/302.
- [26] I. Z. Kiss, Y. Zhai, and J. L. Hudson. Emerging coherence in a population of chemical oscillators. *Science*, 296(5573):1676–1678, 2002. doi:10.1126/science.1070757.

- [27] Y. Kuramoto. *Chemical Oscillations, Waves, and Turbulence*. Springer, 1984.
- [28] J. Lavaei and S. H. Low. Zero duality gap in optimal power flow problem. *IEEE Transactions on Power Systems*, 27(1):92–107, 2012. doi:10.1109/TPWRS.2011.2160974.
- [29] J. M. Lee. *Introduction to Smooth Manifolds*. Springer, 2003.
- [30] E. Mallada, R. A. Freeman, and A. K. Tang. Distributed synchronization of heterogeneous oscillators on networks with arbitrary topology. *IEEE Transactions on Control of Network Systems*, 3(1):1–12, 2016. doi:10.1109/TCNS.2015.2428371.
- [31] D. C. Michaels, E. P. Matyas, and J. Jalife. Mechanisms of sinoatrial pacemaker synchronization: A new hypothesis. *Circulation Research*, 61(5):704–714, 1987. doi:10.1161/01.RES.61.5.704.
- [32] R. E. Mirollo and S. H. Strogatz. The spectrum of the locked state for the Kuramoto model of coupled oscillators. *Physica D: Nonlinear Phenomena*, 205(1-4):249–266, 2005. doi:10.1016/j.physd.2005.01.017.
- [33] P. Monzón and F. Paganini. Global considerations on the Kuramoto model of sinusoidally coupled oscillators. In *IEEE Conf. on Decision and Control*, pages 3923–3928, San Diego, USA, December 2005. doi:10.1109/CDC.2005.1582774.
- [34] Y. Moreno and A. F. Pacheco. Synchronization of Kuramoto oscillators in scale-free networks. *Europhysics Letters*, 68(4):603, 2004. doi:10.1209/epl/i2004-10238-x.
- [35] T. Nishikawa, A. E. Motter, Y. C. Lai, and F. C. Hoppensteadt. Heterogeneity in oscillator networks: Are smaller worlds easier to synchronize? *Physical Review Letters*, 91(1):14101, 2003. doi:10.1103/PhysRevLett.91.014101.
- [36] J. Pantaleone. Stability of incoherence in an isotropic gas of oscillating neutrinos. *Physical Review D*, 58(7):073002, 1998. doi:10.1103/PhysRevD.58.073002.
- [37] V. Rakočević. On continuity of the Moore-Penrose and Drazin inverses. *Matematički Vesnik*, 49(3-4):163–172, 1997. URL: <http://www.emis.de/journals/MV/9734>.
- [38] G. S. Schmidt, A. Papachristodoulou, U. Münz, and F. Allgöwer. Frequency synchronization and phase agreement in Kuramoto oscillator networks with delays. *Automatica*, 48(12):3008–3017, 2012. doi:10.1016/j.automatica.2012.08.013.
- [39] R. Sepulchre, D. A. Paley, and N. E. Leonard. Stabilization of planar collective motion: All-to-all communication. *IEEE Transactions on Automatic Control*, 52(5):811–824, 2007. doi:10.1109/TAC.2007.898077.
- [40] J. W. Simpson-Porco, F. Dörfler, and F. Bullo. Synchronization and power sharing for droop-controlled inverters in islanded microgrids. *Automatica*, 49(9):2603–2611, 2013. doi:10.1016/j.automatica.2013.05.018.
- [41] P. A. Tass. A model of desynchronizing deep brain stimulation with a demand-controlled coordinated reset of neural subpopulations. *Biological Cybernetics*, 89(2):81–88, 2003. doi:10.1007/s00422-003-0425-7.
- [42] M. Verwoerd and O. Mason. Global phase-locking in finite populations of phase-coupled oscillators. *SIAM Journal on Applied Dynamical Systems*, 7(1):134–160, 2008. doi:10.1137/070686858.
- [43] M. Verwoerd and O. Mason. On computing the critical coupling coefficient for the Kuramoto model on a complete bipartite graph. *SIAM Journal on Applied Dynamical Systems*, 8(1):417–453, 2009. doi:10.1137/080725726.
- [44] Y. Wang and F. J. Doyle III. Exponential synchronization rate of Kuramoto oscillators in the presence of a pacemaker. *IEEE Transactions on Automatic Control*, 58(4):989–994, 2013. doi:10.1109/TAC.2012.2215772.
- [45] N. Wiener. *Nonlinear Problems in Random Theory*. MIT Press, 1958.
- [46] A. T. Winfree. Biological rhythms and the behavior of populations of coupled oscillators. *Journal of Theoretical Biology*, 16(1):15–42, 1967. doi:10.1016/0022-5193(67)90051-3.
- [47] R. D. Zimmerman, C. E. Murillo-Sánchez, and R. J. Thomas. MAT-POWER: Steady-state operations, planning, and analysis tools for power systems research and education. *IEEE Transactions on Power Systems*, 26(1):12–19, 2011. doi:10.1109/TPWRS.2010.2051168.



**Saber Jafarpour** (M'16) is a Postdoctoral researcher with the Mechanical Engineering Department and the Center for Control, Dynamical Systems and Computation at the University of California, Santa Barbara. He received his Ph.D. in 2016 from the Department of Mathematics and Statistics at Queen's University. His research interests include analysis of network systems with application to power grids and geometric control theory.



**Francesco Bullo** (IEEE S'95-M'99-SM'03-F'10) is a Professor with the Mechanical Engineering Department and the Center for Control, Dynamical Systems and Computation at the University of California, Santa Barbara. He was previously associated with the University of Padova, the California Institute of Technology, and the University of Illinois. His research interests focus on network systems and distributed control with application to robotic coordination, power grids and social networks. He is the coauthor of *Geometric Control of Mechanical Systems* (Springer, 2004) and *Distributed Control of Robotic Networks* (Princeton, 2009); his forthcoming "Lectures on Network Systems" is available on his website. He received best paper awards for his work in IEEE Control Systems, Automatica, SIAM Journal on Control and Optimization, IEEE Transactions on Circuits and Systems, and IEEE Transactions on Control of Network Systems. He is a Fellow of IEEE and IFAC. He has served on the editorial boards of IEEE, SIAM, and ESAIM journals, and serves as 2018 IEEE CSS President.